ACCESSIBILITY

OsloMet – Oslo Metropolitan University

Department of Civil Engineering & Energy Technology

Section of Civil Engineering

Master Program in Structural Engineering & Building Technology

MASTER THESIS

TITLE OF REPORT	**DATE**
Salt-Flavored Green Binder (SAF^{GB}): Focus on Flowability, Microstructure and Strength	Mai 25th 2023
	PAGES / ATTACHMENTS 49
AUTHOR(S) Mahmoud Alizadeh Farshchian	**SUPERVISOR(S)** Sarra Drissi,

SUMMARY / SYNOPSIS

This thesis investigated the combined effect of seawater and Supplementary Cementitious Materials (SCMs) on the compressive strength of cement paste. The study explored various binders with different proportions of silica fume and fly ash at a constant seawater to binder ratio in order to understand the relationship between these factors and the resulting compressive strength. Flowability, hardened density and the microstructure of the different studied mixtures were examined in order to explain the observed variation in the compressive strength. No clear trend was observed in the compressive strength of different mixture. Similar results were noticed after applying up to 108 thermal cycles. In general, the increase of SCMs up to 30% resulted in lower compressive strength regardless of the type of water used.

KEYWORDS
Green binder
Strength
Microstructure

Acknowledgement

This master's thesis was conducted at Oslo Metropolitan University during the spring of 2023 as a significant component of the Structural Engineering and Building Technology master's Program. The primary objective of this thesis is to investigate the impact of seawater on cementitious materials, aiming to gain a comprehensive understanding of its effects on the behavior of cement-based materials. Additionally, it seeks to explore the potential advantages of substituting freshwater with seawater in the cement industry.

I would also like to express my gratitude to the following individuals who have contributed to and supported me in this endeavor:

- Ingrid Gigstad: For generously providing the necessary manuals and materials for conducting the FTIR test.
- Dimitrios Kraniotis: For providing invaluable assistance in the Energy and Building Technology Lab.
- Rafael Borrajo and Rune Orderløkken: Providing assistance with FTIR testing.
- Simen Antonsen: providing guidelines using the the FTIR machine.
- Nilsen Ledermann: Preparing instruments, providing user's manual and the preparation of test materials at Energy and Building Technology lab.

And my gratitude to Sarra for supervising.

Abstract

The construction industry is expanding rapidly as a result of global economic expansion, resulting in increasing demand for and production of building materials. Regrettably, this expansion contributes significantly to CO2 emissions, mainly from the cement industry. Furthermore, it increases the lack of natural resources and the scarcity of fresh water. Given these obstacles, it is critical to investigate more efficient methods of producing environmentally friendly construction materials.

In response to the previous problems in the concrete industry, this study suggests the manufacture of a sustainable and innovative cement paste. The proposed method comprises replacing a significant percentage of cement with a low-carbon binder, such as fly ash or microsilica (about 20% and 30%, respectively). In addition, seawater will be utilized in place of freshwater. By combining these components, a green and salt-flavored cement paste with ecological and economic benefits may be created.

To cost-effectively predict and optimize the properties (mainly compressive strength) of paste made from any combination of the binders, several models and corresponding iso-term contours will be defined from experimental data of several mixture proportions selected by statical design method in a system consisting of 70-100% cement, 10-20% fly ash and 0-10% microsilica. The accuracy of the models will be checked by comparing the predicted and experimental properties of some mixtures selected within the system boundaries. To quantify the feasibility of producing a green and unreinforced salt-flavored paste, the changes in the properties of the paste, subjected to several freeze-thaw cycles to mimic the long-term natural aging process of the mortar, in the forms weight loss, compressive strength and microstructure will be examined.

Contents

List of figures.

List of Tables.

Abbreviations.

Abbreviation	Meaning
SCM	Supplementary Cementitious Materials
FW	Freshwater
SW	Seawater
TW	Tap water
FTIR	Fourier transform infrared
SEM	Scanning electron microscope
GCCA	Global cement concrete association
UN	United Nations
GGBS	Ground Granulated Blast-furnace Slag
OPC	Ordinary Portland Cement
CEM	Cement
SAF^{GB}	Salt-Flavored Ternary Binder
CBM	Construction and building material
Prisma	systematic reviews and meta-analyses
SF	Silica fume
FA	Fly ash
MK	Metakaolin
GP	Glass powder
LM	Limestone
DW	deionized water
BFS	Blast furnace slag
C-S-H	calcium-silicate-hydrate
SP	Superplasticizers
W/b	Water to binder ratio
W/c	Water to cement ratio
PCM	Phase Change Material
ASTM	American Society for Testing and Materials

Chapter 1: Introduction

1. 1. Context

Concrete is the most commonly used building material worldwide, but its production is associated with significant consumption of natural resources [1]. In 2020, 14 billion m^3 concrete was produced in 2020 as reported by GCCA leading to an enormous water consumption [2]. Fig. 1 illustrates the amount of fresh water (FW) used in concrete production in UK and China. It is clear that there is a clear reduction trend of FW consumption associated with concrete production in UK while the FW consumption per capita in China continue to increase. FW is not only used for mixing, placing and curing of concrete, but it is also important for other stages of concrete production such as washing during the extraction of aggregates, and cleaning concrete tracks and plants, etc. In recent years, the environmental concerns and the global FW scarcity crisis have led to increased interest in alternative Portland cement and water sources for concrete production. According to the UN, 2.2 billion people lack access to FW, and this figure is expected to rise as a result of climate change and population growth [3].

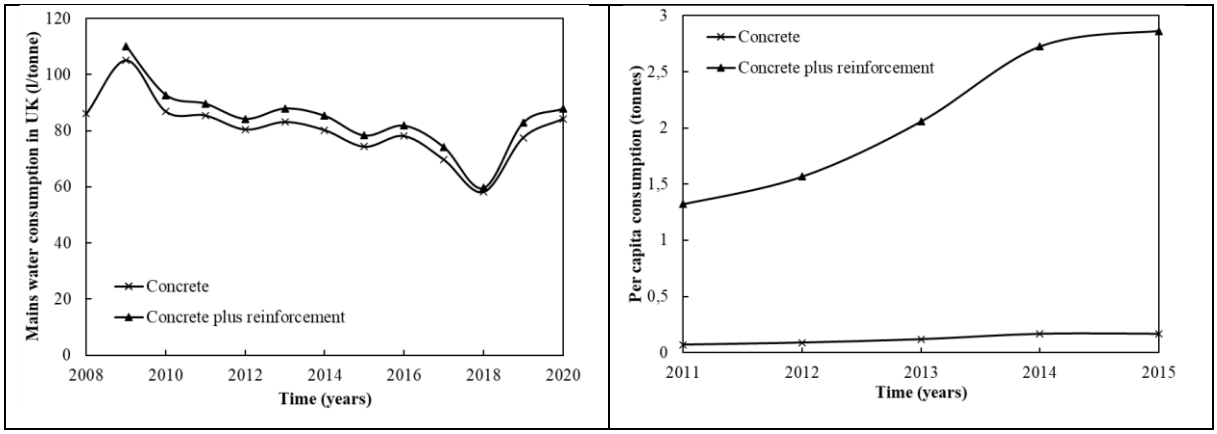

(a) (b)

Fig1. 1. Fresh water consumption in (a) UK [4] and (b) China [5] for ready mixed concrete.

Therefore, the concrete industry should find alternative sources for FW. One such option is the use of non-potable water, such as seawater (SW). For instance researchers in this study [6] observed a 26% and 21% reduction of CO_2 emission by using fly ash and GGBS as a replacement alternative for OPC. In the research paper Li et al. [7] considered the demand of concrete for freshwater. It stated that concrete uses over two billion tons of freshwater, therefore replacing freshwater with seawater is quite beneficial. The use of SW in concrete goes back to the early ages in ancient Romans [8]. Similarly, recent studies have demonstrated again the

feasibility of using SW in concrete [9, 10]. Ahmed et al. [11] reported a 2% increase in strength of concrete mixed with SW over FW. Moreover, Mohammed et al. [12] demonstrated that using SW generates a faster strength development after 28 days than using FW, which was attributed to an improvement in the microstructure of concrete due to the accelerated hydration by the presence of chloride. Another study by Younis et al. [13] concluded that SW accelerate the strength development and tensile strength at early age. There has been observed strength increasement of concrete at the early ages (3 and 7 days) by implanting seawater as a mixing water.

Another significant challenge faced by the concrete industry is its substantial carbon dioxide (CO_2) emissions. The production of cement (CEM) alone accounts for over 10% of annual CO_2 emissions [14]. To address this issue, there has been a growing interest in utilizing Supplementary Cementitious Materials (SCMs) in concrete. However, the use of certain SCMs, such as fly ash (FA), can have a detrimental effect on hydration and the early strength development of concrete. Conversely, other SCMs like silica fume or limestone exhibit contrasting effects. In light of these challenges, combining SCMs with seawater presents a promising solution for the concrete industry while overcoming the negative effect of individual SCMs on the properties of cement-based materials.

1.2. Research gaps and novelty

Over the past two decades, several studies have been conducted on the individual and combined use of SCMs and SW in cement-based materials. Surprisingly, despite Norway's extensive coastline, no relevant research has been undertaken in the country regarding this specific topic. To the best of our knowledge, only two studies conducted by Weerdt et al. [15, 16] have explored the impact of seawater on the properties of 100% Portland cement paste. Considering the growing adoption of blended and low carbon cement in Norway, the utilization of SW-blended cement binders presents an appealing alternative to conventional concrete in the construction industry.

On the other hand, it is widely recognized that the individual application of SF and SW can effectively enhance the early age strength of cement-based materials [17, 18], thereby mitigating the significant impact of Fly Ash (FA) on the early age strength development [17]. However, there is a lack of studies examining which material, SF or SW, exerts a dominant influence on the early strength when they are combined together.

Furthermore, the focus of available studies has been mostly placed on hydration, compressive strength, shrinkage, chloride binding and corrosion of cement-based materials

mixed with SW. For a successful implementation of this technology in Norway, it is crucial to investigate the freeze thaw resistance of this binder. This would provide a valuable insight on the properties of SW-cement based materials following thermal cycling, offering a comprehensive understanding of their durability in challenging winter conditions.

a1.3. Research Questions

The research questions this thesis will try to answer are: (1) What is already known about the individual and combined effect of SW, SF and FA on the properties of cement-paste?, (2) Can SCMs be beneficial for the compressive strength of a paste made with SW or will they introduce a more complex effect?, (3) Is the microstructure sufficient to explain the strength variation of a paste containing both SCMs and SW? (4) Which of the SF or SW exerts a dominant influence on the strength variation of the paste at early age? and (5) Will the studied binder maintain its strength after undergoing multiple thermal cycling?

1.4. Objective

The main objective of this study is to understand how the presence of SW, SF and FA affect the early and later age strength of cement-paste. The aim is to acquire an in-depth knowledge required to optimize and promote the combined use of seawater and SCMs in concrete, in particular for marine and coastal applications. The variation in compressive strength is interpreted through the investigation the fresh properties (flow and slump) and microstructure (FTIR and SEM) as well as the density, water absorption and voids of different mixes after the curing process and thermal cycling. It is crucial to emphasis that the corrosion behavior of the studied binders was not within the scope of this study, as its focus lies in the application of non-reinforced concrete blocks and the construction of structures directly exposed to seawater in coastal and marine areas. Consequently, establishing a comprehensive understanding of the impact of seawater on the binder takes precedence over investigating durability aspects.

1.5. Limitations

This project has been fortunate to receive extensive help and support from various individuals at OsloMet. However, several limitations and challenges have been encountered and need to be outlined:

1.5.1. Time limitation

MABY 5900 (Master thesis) at Oslomet is scheduled to start at the beginning of each spring semester. However, due to the research stay in the USA and necessary time for resettling, this work didn't begin until March.

1.5.2. Restricted access to concrete laboratory

One of the most significant challenges that impacted on the overall timeline of this project is the limited access to the Lab. For instance, the Lab engineer imposed severe and illogical restrictions, allowing only one group to enter and use lab. In addition, experiments were not allowed to be carried out during lab course. Consequently, the progress of experiments was considerably impacted. On the other hand, the lab engineer imposed a strict requirement of always having a lab assistant present. While these regulations are essential for ensuring safety, it posed a substantial challenge as they prevented the student from working independently and placed a substantial burden on the supervisor's time.

1.5.3. - Lack of equipment, tools, materials, and chemicals

Another challenge that hindered conducting an in-depth investigation of the proposed project is the lack of equipment, tools, and chemicals at OsloMet. For instance, the lack of a cement paste mixer resulted in the use of a kitchen blender. While the use of a kitchen blender for paste has been reported in previous studies, it proved to be problematic in this project. The used mixer was subjected to excessive heating when a low w/b ratio (0.15) was considered in the initial stage of this project, leading to the modification of the mix design. Also, a big variability was noticed in the compressive strength results, potentially attributed to the inability of the mixer to mix the paste thoroughly and homogeneously. It is important to note that visually, all fresh mixes appeared to be homogeneous. On the other hand, the lack of necessary chemicals (isopropanol), materials (SW), storage bottles, vacuum ovens, and vacuum desiccators and missing equipment' cables presented additional challenges. Therefore, the project had to proceed using the available resources in the lab or required the supervisor to purchase the necessary items. In addition, it was the student who personally collected the SW from Indre Oslo fjord that was needed for this project.

1.5.4. - Lack of Communication

The smooth progress of the project was hindered by the ineffective communication among certain Profs at OsloMet. This led to significant problems, including instances of items being removed or borrowed from the lab without prior notification. Consequently, the scheduled thermal conductivity tests had to be canceled, despite the efforts made to cast special molds in the 3D department and prepare samples for testing.

1.5.5. - Lack of experience and expertise

The lack of expertise in handling lab equipment complicated the execution of the work. Moreover, the lack of experience with mixing a paste with an extreme low w/b ratio added to the complexities of the project. This presented obstacles in achieving the desired outcomes and hindered the smooth progression of the work.

Despite the limitations and thanks to the invaluable guidance, help and assistance of the supervisor of this thesis, it is considered that the goal of the thesis has been accomplished. However, it is strongly recommended that OsloMet proactive measures to address these challenges to provide a comfortable and supportive work environment for students. By doing so, it will foster students' motivation to use the different labs effectively and thus enabling them to contribute towards finding solutions to the challenges faced by the construction industry in Norway.

1.6. Thesis outline

This thesis is divided into 5 chapters, as depicted in Fig. 1.1. The introduction, objectives and limitations of the conducted work are presented in Chapter 1. The aim was to introduce the research topic, identify existing research gaps, define and limit the scope of the investigation and provide an overview of what lies ahead. In Chapter 2, a comprehensive state of the art review is presented, consolidating the knowledge relevant to this topic. This chapter along with visits to labs (concrete lab, energy lab, chemistry lab and MEK lab) at OsloMet allowed us to shape the experimental work detailed in Chapter 3. Chapter 4 summarizes and discusses the key findings of this work. Finally, Chapter 5 offers concluding remarks and outlines potential avenues for future work. As a result of this study, a manuscript is being written based on the findings of this study and will be submitted to Construction and Building Materials (CBM) journal in the coming days.

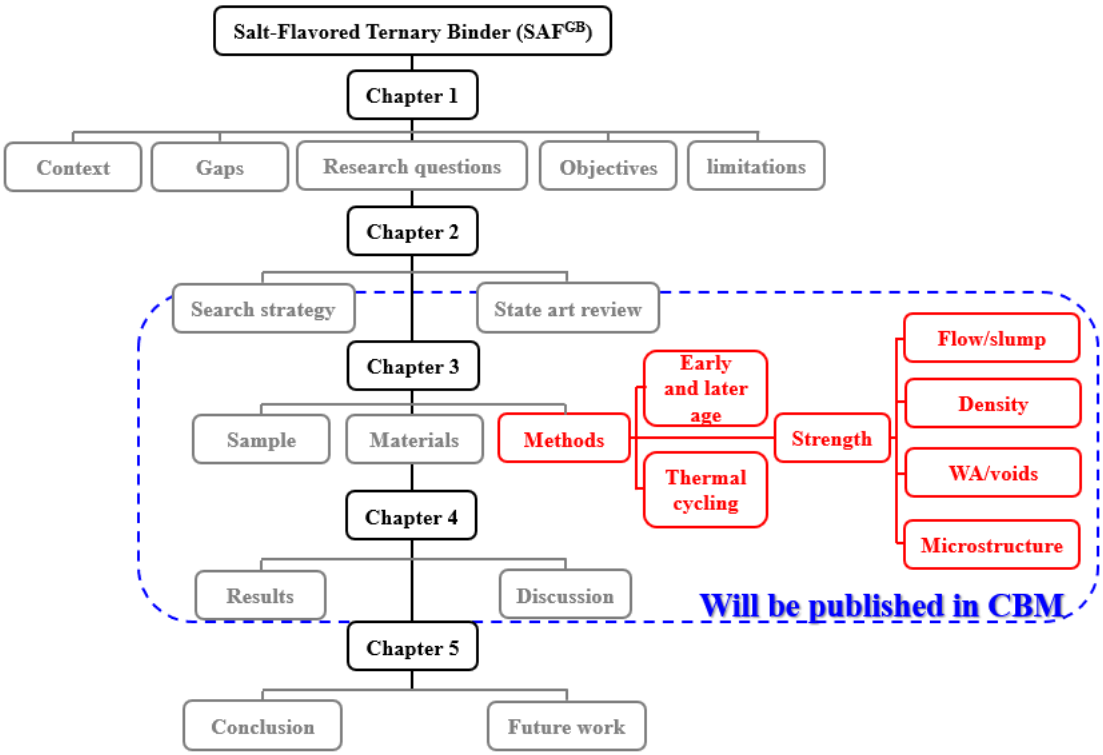

Fig1. 2. A flow chart of the thesis structure.

Chapter 2: Literature review

2.1. Introduction.

In this chapter, a comprehensive literature review will be presented, focusing on the analysis of studies and research conducted by other scholars to enhance our understanding of the subject matter. Careful selection of relevant literature was undertaken to ensure a deeper comprehension of the topic at hand. Throughout the process of literature selection, various strategies and techniques were employed to optimize time utilization and enhance the effectiveness of the search process.

2.2. Literature search strategy

A systematic review was done in order to meet the goals for this paper. It is an efficient method for locating material pertinent to a study subject. Then, this collection of material is compiled and reviewed to identify questions and knowledge gaps that might direct future study. [19]

Based on the Recommended Reporting Items for Systematic Reviews and Meta-Analyses (PRISMA) method's criteria, this systematic review was carried out [19] and summarized In Figure 1. It is based on the following research questions: What is the effect of fly ash on cement's paste? What is the effect of micro silica on cement's paste? What is the effect of seawater on cement's paste? What is the mixture effect of seawater and fly ash on cement's paste? What is the mixture effect of micro silica and seawater on cement's paste? Therefore, a search was done in the Scopus database using a combination of keywords relating to seawater cements, bound by the Boolean operator AND. The OR operator enabled the listing of journal articles cited and recorded in this paper. Thus, the chosen search term corresponded to: ("Fly ash" OR "Micro silica" OR "Seawater") AND ("Cement's paste" OR "Cement" OR "Silica Fume" OR "Mortar" OR "Fly ash" OR "Mixture" OR "Effect"))). The search was restricted to English article titles.

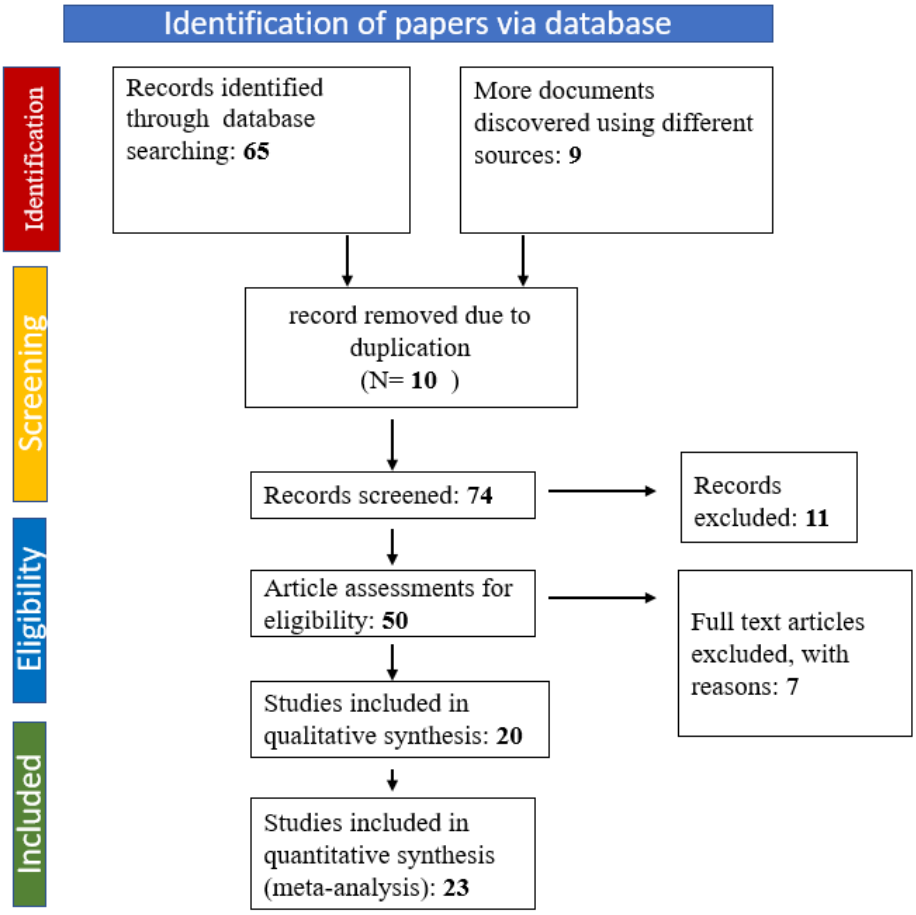

Fig 2. 1 Systematic literature review flowchart. Adapted from[19].

2.3. Selection criteria.

The following inclusion criteria were used for screening: "the effect of seawater on cement" in the study had to be used (rather than, say, a seawater effect on concrete or seawater effect on reinforced concrete); Seawater had to partially replace the use of freshwater in cement mix. For the sake of simplicity in this paper, we neglected the effect of seawater on reinforced concrete or overall concrete's behavior in marines' area.

2.4. Data extraction.

The following content was retrieved from each paper: 1) characteristic of cement's paste mixed with seawater. 2) characteristics of seawater mixed with fly ash. 3) characteristics of sweater mixture with SF. 4) effect of fly ash on cement 5) effect of seawater on behaviour of concrete at early ages. 6) micro structural analysis of seawater cement paste

2.5. The combined effect of seawater, FA and SF on cement.

There have been several studies conducted on the effect of seawater on the cementitious material. Studies such as comparison between cement mixed with seawater and cement mixed with freshwater, effect of seawater cement's early age behavior, microstructural analysis.

For instance, in a study conducted by Zhou et al [20] comparison between cement paste mixed with deionized water and cement paste mixed with seawater with w/b 0.5, was made. Seawater samples exhibited initial higher hydration rate compared to other samples. Authors of this study observed also finer C-S-H nuclei on surface of seawater's clinker particle then deionized water samples.

In other study conducted by Katano et al [21]. Conducted a comparison test on foot-protection blocks with 45% water to binder ratio. Later on, he discovered that samples mixed with seawater exhibited a higher strength then those mixed with fresh water at the early ages. **Error! Reference source not found.** shows the further results on the experiments and c omparison between seawater and freshwater samples at different age.

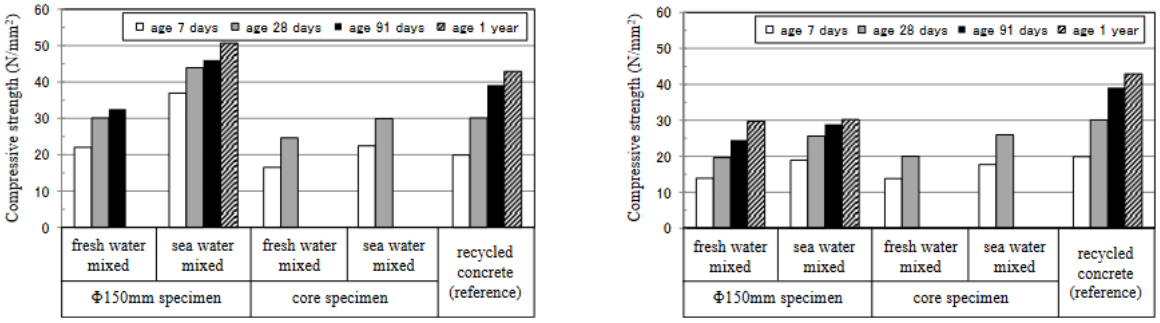

Fig.2. 1. Compressive strength results [21].

Several researchers have discovered that incorporating seawater as a mixing water in concrete induces alterations in the strength development of the matrix. For instance, use of seawater results a strength gain and reduction of setting time at the early ages [12]. Furthermore, Li et al [22]. Conducted a study focused on investigating the early age hydration of seawater in the presence of slag, SF (silica fume), and cement with a low water binder ratio. The researcher observed that the utilization of seawater led to an accelerated hydration process in the ternary mixture of slag and SF. Furthermore, seawater usage contributed to an increase in the overall heat generation compared to samples mixed with freshwater **Fig.2. 2** .

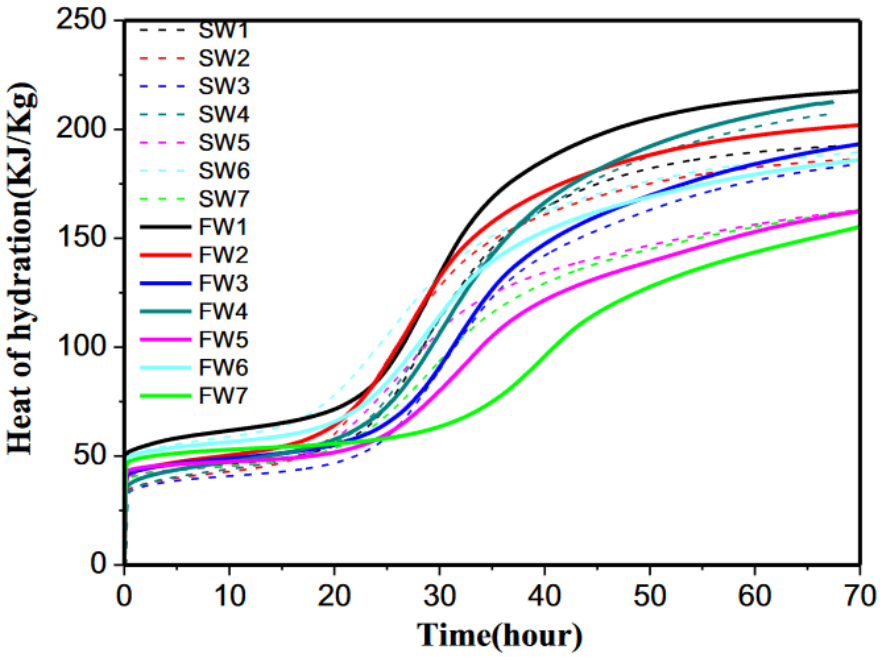

Fig.2. 2. Heat of hydration vs time [22].

Furthermore Li et al [22], discovered that samples with seawater after 3 days of curing, exhibited a higher compressive strength compared to other samples. This improvement was particularly noteworthy in mixtures containing slag **Fig.2. 3**. The study's conclusion demonstrated that the utilization of seawater had a significant influence on the strength development of cement and slag. Furthermore, the effects of seawater on the formation of calcium-silicate-hydrate (C-S-H) differed between specimens containing slag and those containing silica fume (SF). Seawater promoted the formation of low calcium-to-silicon ratio C-S-H in SF-containing specimens, whereas it resulted in the formation of C-S-H gel with higher calcium-to-silicon ratio in mixtures containing slag.

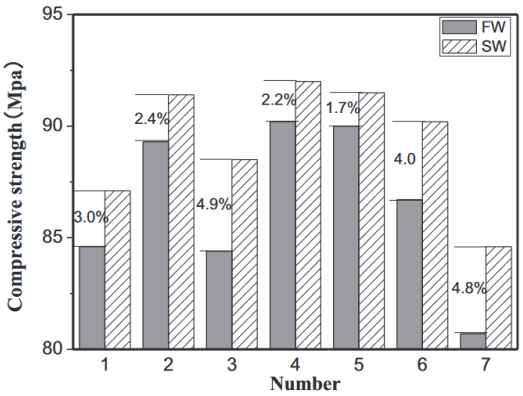

Fig.2. 3. Compressive strength of different past at 3 days [22].

In the other study conducted by Şimşek et al [23] on seawater and freshwater samples with SF substituting 0-15% of cement by weight during casting process of cementitious composites. Researcher discovered that increasing SF dosage resulted in increased water demand for both fresh and seawater sample **Fig.2. 4**. Furthermore, they discovered a delayed setting time by increasing the dosage of SF. However, as the dosage of SF increased, the setting time of cement paste mixed with tap water (TW), experienced a significant delay. Other scholars also reported that by increasing the dosage of SF, workability of the fresh concrete will decrease [24-26]. Moreover, researchers in [23] discovered that the samples mixtures achieved their highest compressive strength values when 10% of silica fume (SF) was used as a replacement, while the lowest values were observed in the control group without any SF replacement (0% SF). Furthermore, the compressive strength values of samples prepared with seawater (SW) were comparable to those prepared with tap water (TW).

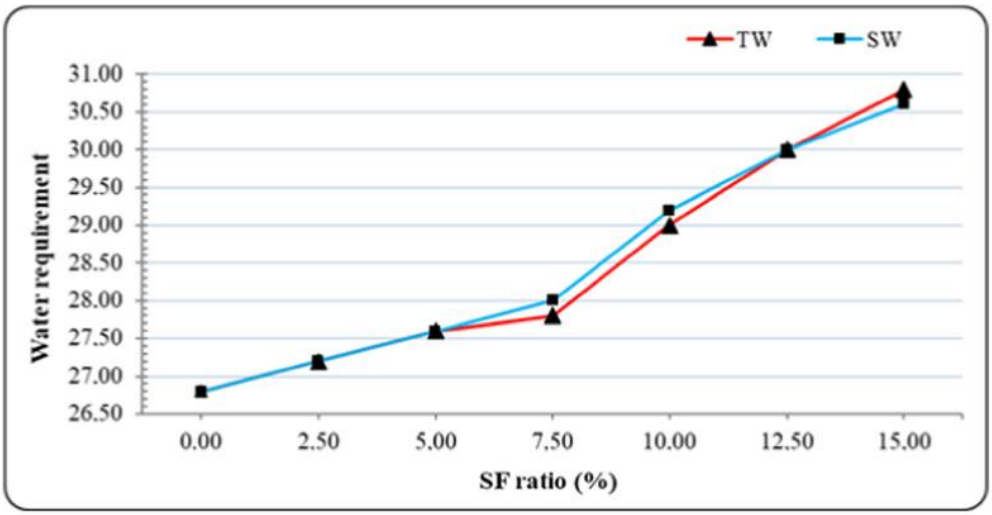

Fig.2. 4. The relation between water demand and SF usage [23].

Moreover, researchers in [27], concluded that the presence of NaCl in seawater affects the binding of calcium hydroxide compounds in concrete. Consequently, this results in the reduction of the calcium hydroxide content in concrete mixed with seawater and moreover this results in increased compressive strength. The continuous reaction between NaCl and Ca(OH)2 leads to the formation of Friedel's salt, which fills the concrete pores and it results in the enhancement of compressive strength. As a result, the compressive strength of concrete mixed with seawater differs from that of concrete mixed with freshwater.

There have been several studies on the effect of seawater on cementitious material. Sikora et al. [10], observed significant difference between seawater samples and demineralized water samples at the early ages. Samples with seawater SW0 (with 100% cement) demonstrated 41% higher strength compared to demineralized water DW0 (100% cement) at the age of 1d **Fig.2. 5** . From this result we can clearly see the positive effect of seawater on the strength of samples at the early ages.

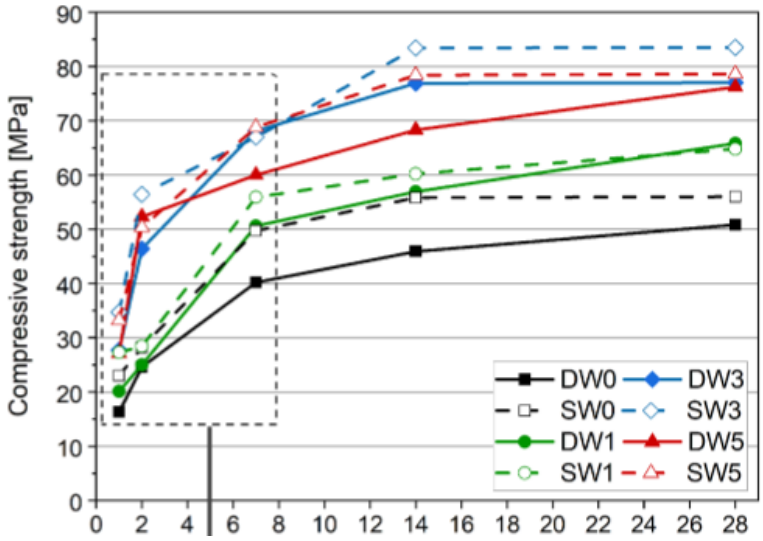

Fig.2. 5. Compressive strength of DW and SW samples [10].

Younis et al [28], also discovered that incorporation of seawater in concrete led to a slight initial increase in both compressive and tensile strength at the 7-day mark. However, a subsequent reduction of approximately 7-10% was observed in both compressive and tensile strengths after 28 days. Moreover, they analyzed the heat flow results for the pastes mixed with freshwater and seawater. They discovered that seawater accelerated the hydration reaction. **Fig.2. 6** shows the results of heat flow for both seawater and freshwater sample in the study conducted by Younis et al.

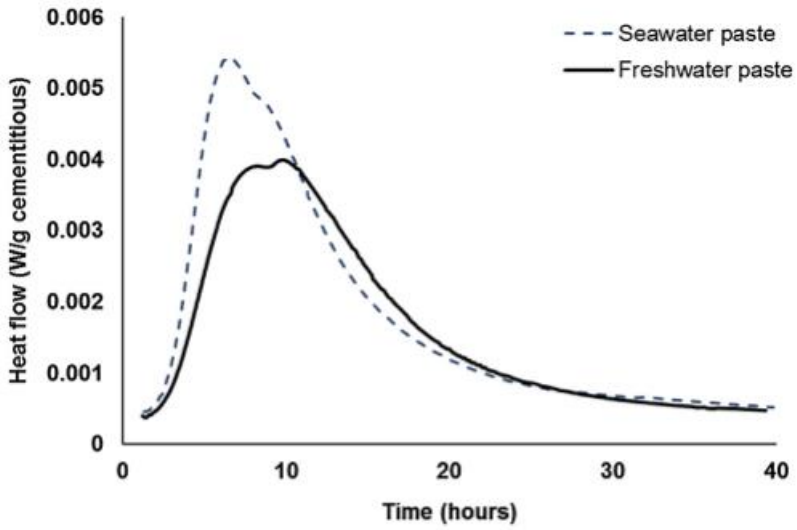

Fig.2. 6. Heat flow effect [28].

Some scholars studied the long-term effect of seawater on concrete. Otsuki et al [29], conducted study over a period of 20 years, in which specimens were rapidly exposed to a tidal environment, revealed that the type of mixing water had negligible impact on the strength of the material. Later on in the literature, authors discuss that the utilization of seawater for mixing increases the reaction ratio of BFS (blast furnace slag) compared to mixing with freshwater throughout the entire period. The highest increase occurs on the first day, followed by a gradual reduction that persists thereafter.

Table.2. 1. Exhibits the test results on fresh properties conducted by Want et al [30]. As it indicates, samples combined with seawater had a negative effect on flowability. Moreover, authors discuss the presence of chlorides in artificial seawater is considered to be the main contributing factor, at least partially to this result. The presence of chlorides in acceleration in the formation of C-S-H (calcium-silicate-hydrate) during the hydration process, resulting in decreasing flowability and reduced excess water. From the table we can observe that seawater had a negative effect on initial and final setting time, this also can be the result of seawater in acceleration of hydration **Fig.2. 7**.

Table.2. 1. Test results on fresh properties of cement mixed with seawater and freshwater conducted by Wang et al [30].

REF	Cement	Fine Aggregates	Silica Fume (SF)	LSP	Natural Zeolite (NZ)	Type of water	W/c	SP (%)	Flow (mm)	Initial set (min)	Final set (min)
[30]	750 (Kg/m3)	990 (Kg/m3)	150(Kg/m3)	200(Kg/m3)	0	Freshwater	0.2	33(Kg/m3)	310	240	260
	750 (Kg/m3)	890(Kg/m3)	150(Kg/m3)	200(Kg/m3)	93.7(Kg/m3)	Freshwater	0.2	33(Kg/m3)	290	225	250
	750 (Kg/m3)	770(Kg/m3)	150(Kg/m3)	200(Kg/m3)	187.3(Kg/m3)	Freshwater	0.2	33(Kg/m3)	280	180	225
	750 (Kg/m3)	990Kg/m3)	150(Kg/m3)	200(Kg/m3)	0	Seawater	0.2	33(Kg/m3)	285	75	110
	750 (Kg/m3)	890(Kg/m3)	150(Kg/m3)	200(Kg/m3)	93.7(Kg/m3)	Seawater	0.2	33(Kg/m3)	275	140	160
	750 (Kg/m3)	770(Kg/m3)	150(Kg/m3)	200(Kg/m3)	187.3(Kg/m3)	Seawater	0.2	33(Kg/m3)	260	140	160

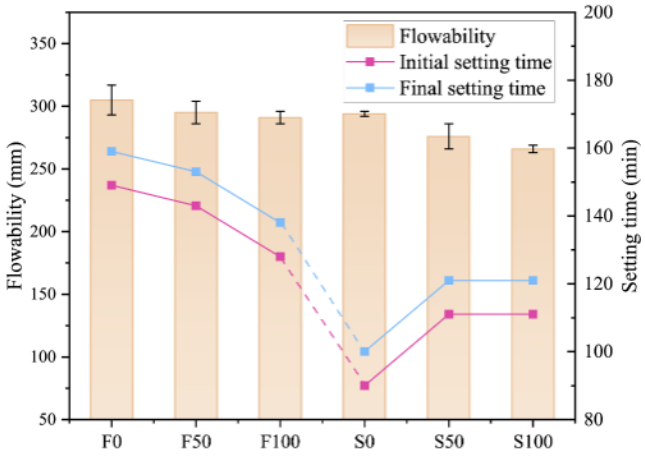

Fig.2. 7. Flowability and setting time, freshwater sample from left to seawater samples to the right [30].

Table.2. 2 demonstrates the results of a comparative study conducted by Huang et al [31] on concrete mixed with seawater and MK. The samples cured under standard conditions were labeled as CMKN for fresh water mixing and SCMKN for seawater mixing. On the other hand, specimens subjected to chloride curing conditions were denoted as CMKC for fresh water mixing and SCMKC for seawater mixing.

The results indicate a general trend of increasing compressive strength with age for most specimens. However, it was observed that CMKC0 and SCMKC0 showed a reduction in compressive strength at 56 days compared to 28 days due to chloride attack. Additionally, for specimens at the same age and under the same curing conditions, the compressive strength exhibited a positive correlation with the MK content **Fig.2. 8**.

Table.2. 2. Study on the effect of seawater on cement by Huang et al [31].

Ref	Cement	Metakaolin	Fine aggregate	Coarse aggregate	Type of water	W/b	SP (%)	Curing methods	Compressive strength (days)		
									3	28	56
[31]	420,0	0	644	1146	Fresh water	0,45	0	Air cured under temperature of 20 °C and relative humidity above 90 and cured in saturated Ca(OH)2 solution with 5 wt% NaCl addition at 20 °C	**35,1**	**45.92**	**51,06**
	411,6	8,4	644	1146		0,45	0		**37,0**	**52.33**	**53,08**
	407,4	12,6	644	1146		0,45	0		**38,2**	**55.24**	**56,58**
	403,2	16,8	644	1146		0,45	0		**39,9**	**54.03**	**57,1**
	399,0	21	644	1146		0,45	0		**44,7**	**61.32**	**60,93**
	394,8	25,2	644	1146		0,45	0		**43,5**	**60.09**	**60,22**
	420,0	0	644	1146	Seawater	0,45	0		**46,5**	**56.1**	**59,52**
	411,6	8,4	644	1146		0,45	0		**49,0**	**62.65**	**63,18**
	407,4	12,6	644	1146		0,45	0		**50,3**	**65.16**	**66,34**
	403,2	16,8	644	1146		0,45	0		**50,8**	**67.14**	**69,45**
	399,0	21	644	1146		0,45	0		**52,1**	**69.95**	**74,34**
	394,8	25,2	644	1146		0,45	0		**49,8**	**67.4**	**70,6**

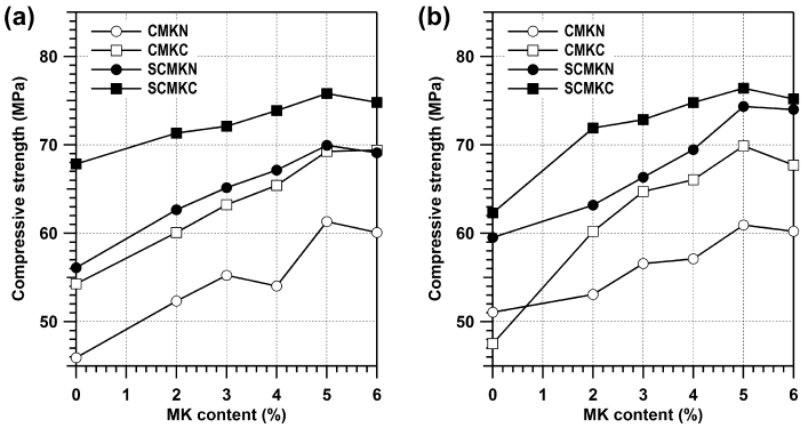

Fig.2. 8. "Strength of concrete with MK content at (a) 28 days, (b) 56 days" [31] .

Table.2. 3, shows the result on hardened properties of cement, a test study conducted by Wang et al [30] Authors of this literature, discovers that cement mixed with seawater exhibits a higher compressive strength compared to sample those mixed with freshwater. However this observation was made for both samples at the same age with presence of zeolite in the mix.

The influence of chlorides in seawater on the hydration process of cementitious materials is evident. Seawater accelerates hydration, leading to a denser microstructure and increased formation of hydration products **Fig.2. 9**.

Table.2. 3. Test results on hardened properties of cement mixed with seawater and freshwater conducted by Wang et al [30]. .

Ref	Cement	Silica	Coarse aggregate	Type of water	W/b	SP (%)	Curing methods	Compressive strength (days)		
								3	28	56
[30]	750 (Kg/m3)	150(Kg/m3)	1190(Kg/m3)	Freshwater	0.2	33(Kg/m3)	standard curing room with a temperature of 20 ± 2 ◦C and a humidity of 90 ± 5%	**80**	**110**	**0**
	750 (Kg/m3)	150(Kg/m3)	1100(Kg/m3)	Freshwater	0.2	33(Kg/m3)		**79**	**115**	**0**
	750 (Kg/m3)	150(Kg/m3)	990(Kg/m3)	Freshwater	0.2	33(Kg/m3)		**78**	**119**	**0**
	750 (Kg/m3)	150(Kg/m3)	1190Kg/m3)	Seawater	0.2	33(Kg/m3)		**85**	**120**	**0**
	750 (Kg/m3)	150(Kg/m3)	1100(Kg/m3)	Seawater	0.2	33(Kg/m3)		**80**	**119**	**0**
	750 (Kg/m3)	150(Kg/m3)	990(Kg/m3)	Seawater	0.2	33(Kg/m3)		**79**	**118**	**0**

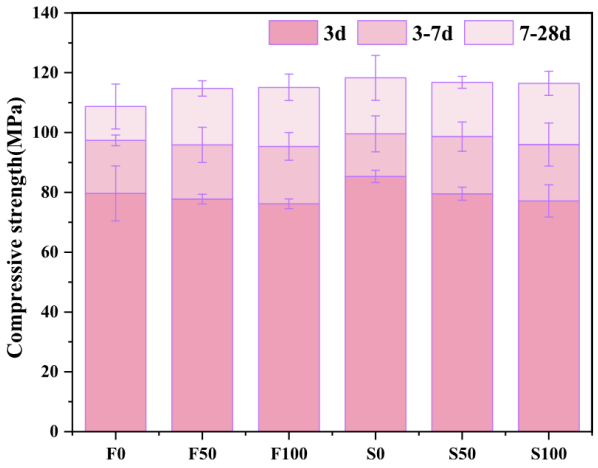

Fig.2. 9. Result of compressive strength, freshwater samples from left to seawater to the right[30].

Table.2. 4, Show the results of research on early age mechanical behavior of Portland cement exposed to seawater by Choi et al [32]. At the age of 7 and 28 days, seawater exhibited beneficial impact on the compressive strength increase. However there has been observed a higher compressive strength for the samples exposed to freshwater compared to samples cured in seawater after 28 days. Furthermore, author discuss that this result may be due to fact that the presence of NaCl in seawater initiates a reaction with hydrated cement, resulting in the generation and subsequent leaching of calcium chloride **Fig.2. 10**.

Table.2. 4. Test results on hardened properties of different admixtures exposed to seawater by Choi et al [32].

Ref	Cement	Metakaolin	Glass powder	Silica	Type of water	W/b	SP (%)	Curing methods	Compressive strength (days)				
									1	7	28	56	90
[32]	95%	0	0	5%	Fresh	0,5	-	Cured in freshwater and cured in seawater	20.26	49.3	54.04	57.57	67.46
	90%	0	0	10%		0,5	-		20.48	53.12	64.42	65.26	71.25
	95%	5%	0	0		0,5	-		21.16	53.16	59.97	69.96	76.42
	90%	10%	0	0		0,5	-		19.51	52.84	66.77	75.56	76.6
	95%	0	5%	0		0,5	-		20.43	48.97	59.6	66.9	72.96
	90%	0	10%	0		0,5	-		16.49	46.94	53.79	65.63	66.67
	95%	0	0	5%	Seawater	0,5	-		20.26	51.07	54.23	55.68	63.2
	90%	0	0	10%		0,5	-		20.48	54.61	62.13	63.24	67.58
	95%	5%	0	0		0,5	-		21.16	54.66	57.09	62.62	73.8
	90%	10%	0	0		0,5	-		19.51	52.83	61.27	64.35	74.75
	95%	0	5%	0		0,5	-		20.43	43.57	53.84	54.49	62.03
	90%	0	10%	0		0,5	-		16.49	41.02	53.12	60.8	65.81

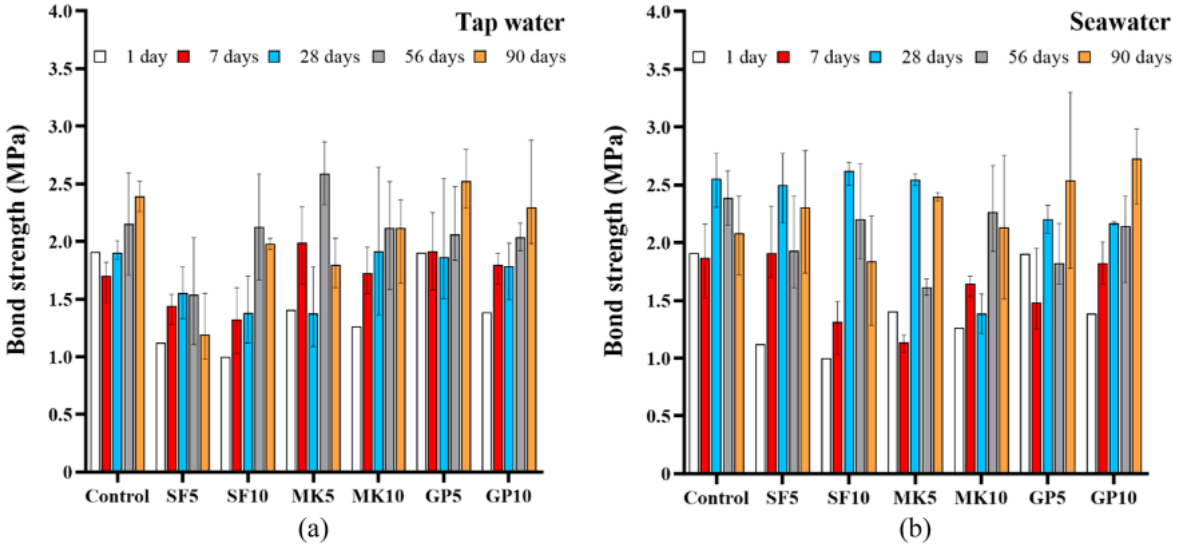

Fig.2. 10. Compressive strength of (a) sample exposed to tap-water, (b) sample exposed to seawater.

Furthermore, author discovered the SF among the additives, exhibited a most effective enhancement in durability compared to other additives such as MK and GP When subjected to seawater, the charge passed through the Portland cement mortars (PCMs) was consistently lower than that in freshwater. Notably, PCMs containing SF exhibited the lowest charge passed, indicating superior performance in terms of durability.

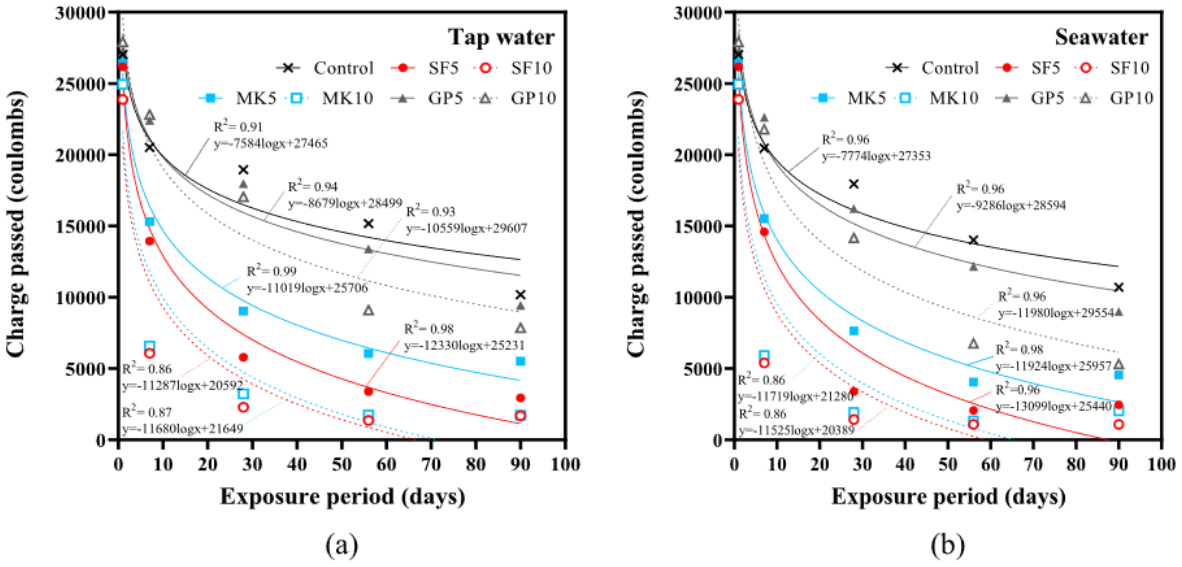

Fig.2. 11. "Charge passed for samples exposed to (a) tap-water and (b) seawater conditions" [32].

Chapter 3: Materials and methods

3.1. Introduction

In this chapter, a comprehensive overview of the materials and experimental techniques used during this project will be presented. Materials and methods were carefully selected to effectively address the research questions raised throughout this project. However, it is important to note that the scope of an in-depth investigation or further experiments was restricted due to the lack of equipment at OsloMet. Therefore, further studies are needed to provide more insight on the kinetics of reaction and microstructure development of the studied binder.

3.2. Materials

3.2.1. Cementitious materials

Industri cement (CEM I 52.5 R) with a Quantile d(95) of 31.30 μm, fly ash (FA) with a typical residue of 16.70% on a 45.00 μm sieve, obtained from NORCEM, and a undensified microsilica Grade 940 U (SF) received from Elkem were used in this study **Fig.3. 1**. The properties of the cementitious materials, provided by the manufacturer, are summarized in **Table.3. 1**,**Table.3. 2**. Based on the data sheet, CEM included 1.99% free lime, and 4.80% limestone. Furthermore, CEM and FA had a density of around 3.13 g/cm^3 and 2.32 g/cm^3, respectively and a specific surface area of 540.00 m^2/kg and 356.00 m^2/kg, respectively.

(a) (b) (c)

Fig.3. 1. Cementitious materials: (a) CEM, (b) FA and (c) SF.

Table.3. 1. Chemical composition of cement and fly ash (wt.%).

	SiO_2	Al_2O_3	CaO	MgO	Fe_2O_3	SO_3	Na_2O	K_2O	P_2O_5	TiO_2	Cl	Other	LOI
CEM	18,96	4,72	61,15	2,29	3,25	3,88	0,428	1,01	0,09	0,30	0,07	3,85	2,95
FA	56,24	22,71	4,44	2,09	6,02	0,4	0,79	1,74	0,68	0,86	0,004	4,03	3,03

Table.3. 2. Properties of SF.

SiO_2 (wt.%)	>90.00
Moisture content (wt.%)	<1.00
LOI (wt.%)	<3.00
Retained on 45μm sieve (wt.%)	<1.50
Bulk density (kg/m^3)	200.00-350.00

The morphology of CEM, FA and SF particles are shown in **Fig.3. 2**. It is clear that the different cementitious materials have distinct morphologies. CEM and SF particles have angular shapes with rough surfaces, while FA exhibits spherical particles with a smooth surface and varying diameters ranging from over 30μm to less than 5μm. Although SF is expected to be spherical, the observation in **Fig.3. 2** (c) shows an agglomeration of the fine spherical, probably due to the SF not being dispersed before SEM analysis and being tested as received. Similar observation was made by Zhang et al [33].

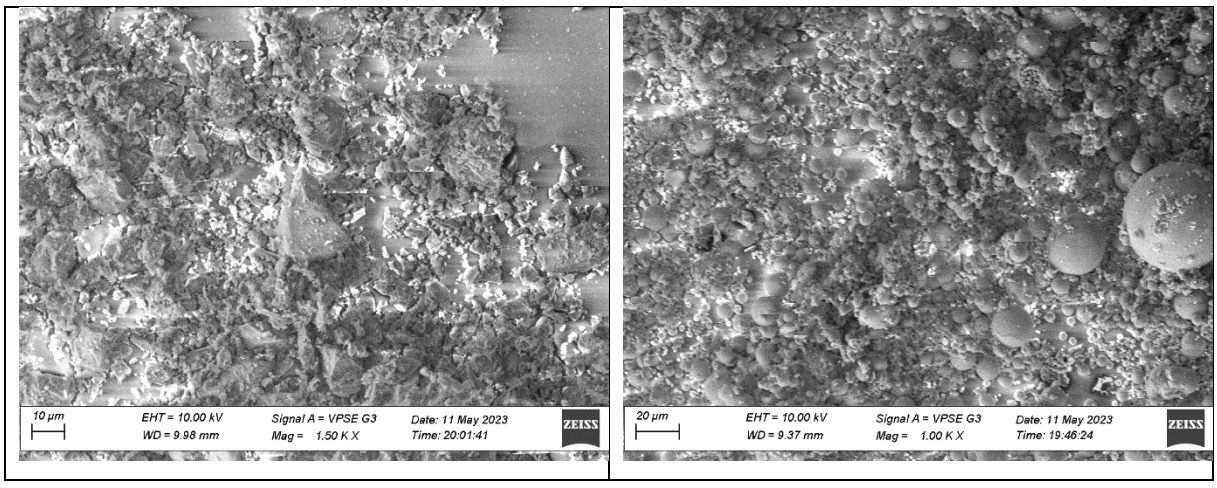

(a) (b)

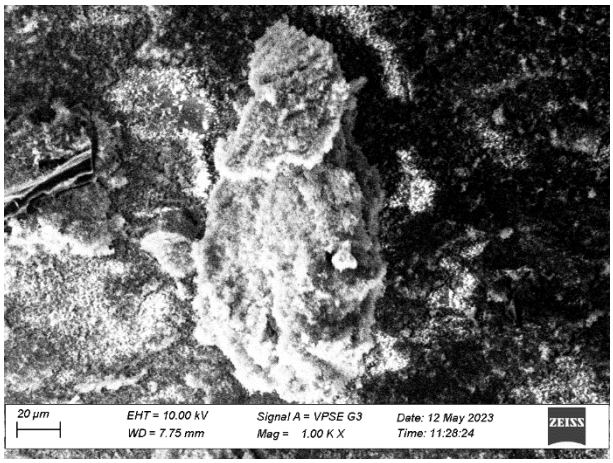

(c)

Fig.3. 2. SEM images of (a) CEM, (b) FA and (c) SF

3.2.2. Mixing water

Seawater (SW), collected directly from Indre Oslo fjord in Norway, was used in this study. SW appears yellow as shown in **Fig.3. 3.** This could be attributed to the dissolved organic matter as reported in [34] and [35]. It has been reported previously that the SW from Indre Oslo fjord exhibit a salinity of 35.00 and its principal constituent are illustrated in **Table.3. 1**[36]. It is clear that the SW is rich of sodium (Na) and chloride (Cl) while its sulfate and magnesium content didn't exceed 8.00% and 4.00%, respectively. Fresh water (FW) was used to prepare the reference samples.

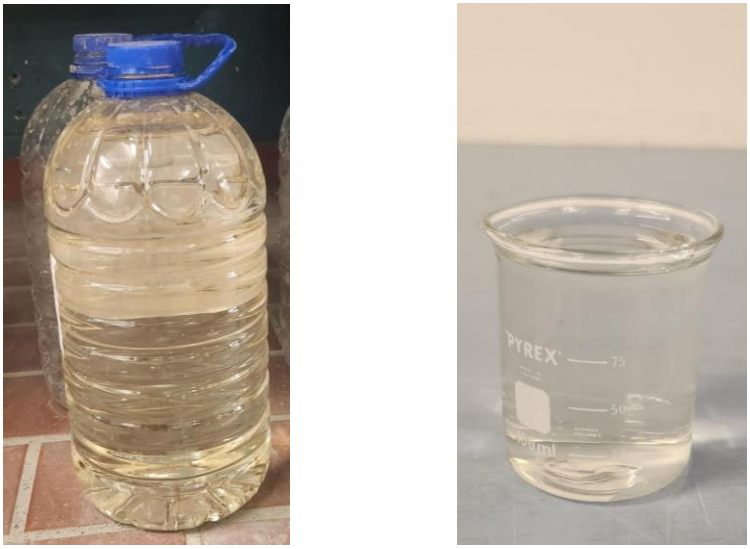

Fig.3. 3. Physical appearance of SW.

Table.3. 3 .Properties of SW (wt.%) taken from [36].

Na^{+}	Mg^{++}	Ca^{++}	K^{+}	Sr^{++}	Cl^{-}	$SO4^{--}$	$NCO3^{-}$	Br^{-}	$BO3^{---}$
30.6	3.7	1.2	1.1	0.04	55.3	7.7	0.4	0.2	0.08

3.3. Sample preparation

The mixture proportions of the studied samples are summarized in **Table.3. 4**. Six different cement pastes with different cementitious content were investigated. FW and SW were used to mix the samples at a constant water to binder (b) ratio of 0.4. A 100% CEM paste with fresh water and seawater was selected as references for other mixtures. The SF replacement level was fixed at 10% by mass of cement in the ternary mixtures while FA content was 10% and 20%.

Table.3. 4. Mix design (wt. %).

ID	CEM	SF	FA	SW/b	FW/b
SW_1	100	0	0	0.4	
SW_2	80	10	10	0.4	
SW_3	60	10	20	0.4	
FW_1	100	0	0		0.4
FW2	80	10	10		0.4
FW_3	60	10	20		0.4

All samples were mixed following ASTM C305 standard [5] at room temperature using a KENWOOD KVL8320S CHEF TITANIUM KJØKKENMASKIN kitchen blender with a variable mixing speed varying from 0 to 666 rpm. Compared to ASTM C305, a higher mixing speed was used in this study primarily based on the suggestion for paste mixing [37, 38] and also in order to disperse the SF particles [38]. The maximum mixing speed of the used blender is 666 rpm. Initially, all powders were pre-mixed for 1min at 140 rpm to homogenize the dry mix. Then, the powder was added to the water and allowed to rest for 30s. Afterward, the mixture was mixed at 266 rpm for 30s and then 326 rpm for 30s and then allowed to rest for 15s. During this time, a rubber spoon was used to scrap down the paste on the side of the bowl. Finally, the mixer was mixed for another 60s at 666 rpm. Immediately after mixing, the paste was poured in $50\times50\times50mm^3$ cubic molds and then cured in sealed conditions for 24h at room temperature. After demolding, the samples were cured in fresh water at around 20°C until the age of testing.

(a) (b)

Fig.3. 4.(a) Kitchen blender, (b) molds.

3.4. Thermal cycling

After 14d of water curing, the hardened cubic samples were subjected to 36, 72 and 108 thermal cycling in a BINDER™ Series MKF dynamic climate chamber **Fig.3. 5**(a). in accordance with ASTM C666, procedure A [39]. The samples were first immersed in a plastic container filled with water and then placed in the chamber to decrease their temperature to approximately 2°C. Once the target temperature is achieved, the freeze-thaw cycles, presented in **Fig.3. 5** (b) were applied. Each freeze thaw cycle took around 4 hours, starting with a thawing in water at a temperature of 4°C for 1 hour and then freezing in a temperature for -10°C for 3 hours at a relative humidity of 98%. The mass loss and the compressive strength of the samples were determined in a thawed condition as specified in the standard [39].

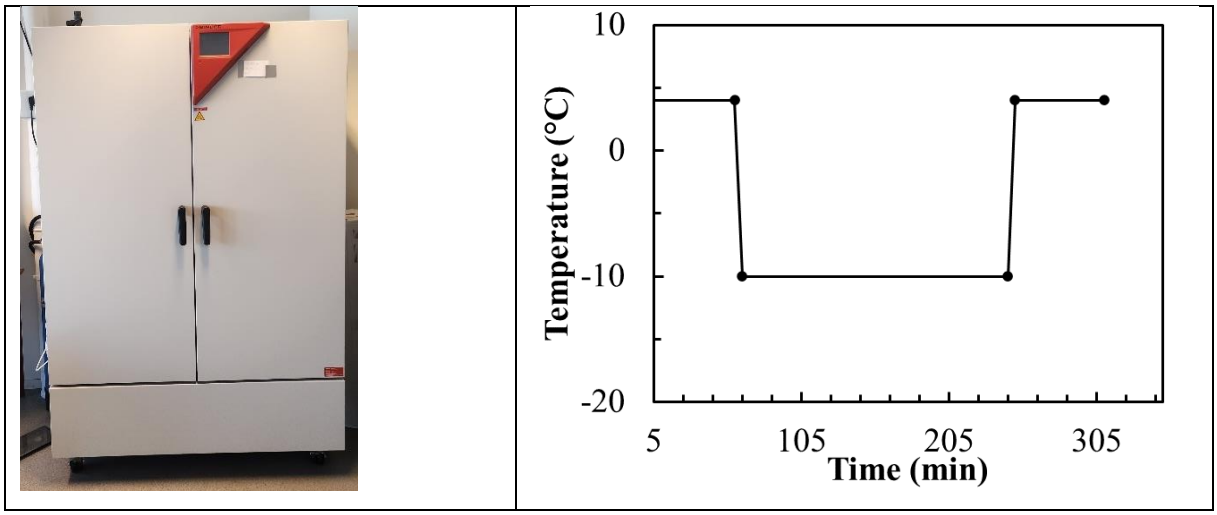

(a) (b)

Fig.3. 5.(a) Climatic chamber and (b) freeze-thaw cycle.

3.5. Methods

3.5.1. Slump and flow

The slump and flow of the samples was determined immediately after mixing as described in [40]. A mini truncated cone mold, as shown in **Fig.3. 6** with a dimension (d×DxH) of 40×90×80 mm^3, was filled with the fresh paste in 2 layers, each approximately the half of the volume of the mold. Each layer was rodded 10 times uniformly. Then, the excess paste was struk off from the surface using a trowel. Finally, the cone was lifted slowly in vertical direction to allow the paste to flow on a flat horizontal plate. The height and diameter of spread were recorded when the flow stopped. The spread was measured by averaging 4 diameters at approximately equispaced intervals.

Fig.3. 6. Truncated cone mold.

3.5.2. Hardened density

Hardened density of the samples were measured in according to ASTM C642 [41]. The hardened densities were calculated from the weighed measurement of cured samples, with a known volume, and the 50mm cubes prior to the compressive strength tests, respectively.

3.5.3. Compressive strength

The compressive strength of the samples after 3d, 28d, 56d of curing and 36, 72 and 108 thermal cycling were determined in triplicates using a Form+test compressive strength machine, **Fig.3. 7**, at a loading rate of 2,25kN/s.

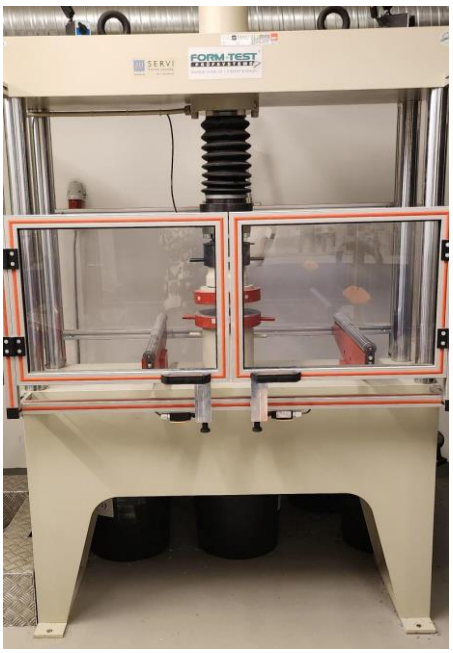

Fig.3. 7. Compressive strength machine.

3.5.4. Water absorption and porosity (voids)

The samples at 3, 28d and after 72 cycles were oven dried in a Termaks series TS9000 oven **Fig.3. 8**(b) and saturated, by immersion and boiling in water, according to the procedure described in ASTM C642 [41]. Eqs. 3.1, 3.2 and 3.3 were used in order to calculate the volume of permeable pore space (voids, v) and the water absorption (Ab_1) after immersion and after immersion and boiling (Ab_2), respectively.

$$v = \frac{g_2 - g_1}{g_2} \times 100 = \frac{C - A}{C - D} \times 100 \qquad 3.1$$

$$Ab_1 = \frac{B-A}{A} \times 100 \quad 3.2$$

$$Ab_2 = \frac{C-A}{A} \times 100 \quad 3.3$$

Where:

g_1 [Mg/m^3] is the bulk density of the sample, dry and is equal to $\frac{A}{C-D}\rho$.

g_2 [Mg/m^3] is the apparent density and is equal to $\frac{A}{A-D}\rho$.

ρ is the density of water = 1Mg/ m^3= 1g/ cm^3.

A [g] is the mass of oven dried sample in air.

B [g] is the mass of surface dry sample in air after immersion.

C [g] is the mass of surface-dry sample in air after immersion and boiling.

D [g] is the apparent mass of sample suspended in water **Fig.3. 8**(a) after immersion and boiling.

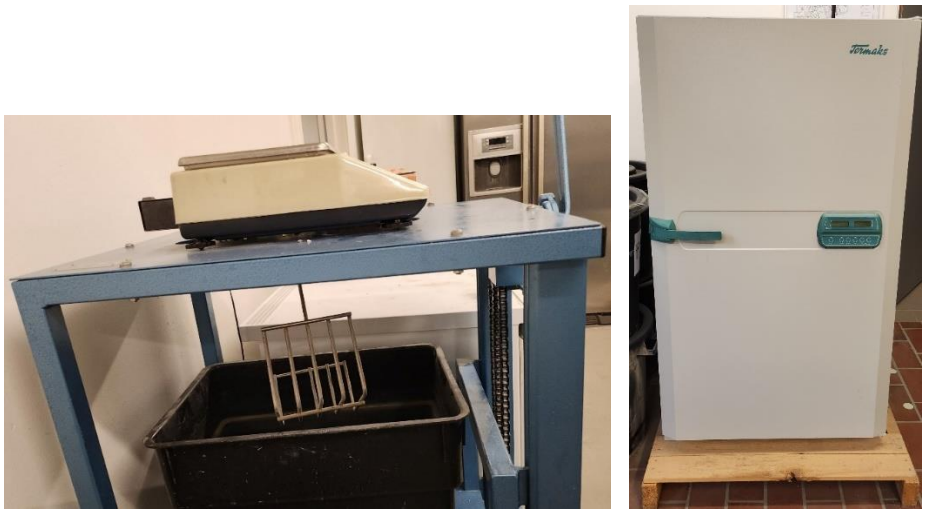

Fig.3. 8.(a) A scale with a connected string (b) Oven.

3.5.6. Mass loss

The mass loss of samples after 36, 72 and 108 cycles was determined by weighing the samples in a thawed condition as detailed in ASTM C666 [39] .Initial weight measurement was taken when the sample temperature reached 2°C prior to applying the freeze-thaw cycles.

3.5.7. Microstructure

3.5.7.1. Hydration stoppage by solvent exchange

Small fragments collected from the core of each sample following the compressive strength tests at 28d, after 72 and 108 cycles were immersed in ethanol for 48h [42]. The ethanol: sample ratio was about 100:1, as shown in **Fig.3. 9**(a). Ethanol was replaced twice during the immersion process. The solvent was removed by drying the sample at 40°C under atmospheric pressure for 48h **Fig.3. 9**(b). Vacuum is not used in this study due to lack of equipment in the laboratory. After drying, the samples were stored in a desiccator **Fig.3. 9**(c) until testing.

(a) (b) (c)

Fig.3. 9. Samples (a) immersed in ethanol (b) placed in the oven at 40°C and (c) stored in a desiccator.

3.5.7.2. Fourier Transform Infrared Spectroscopy

Fourier Transformation Infrared (FT-IR) spectra was obtained using a PerkinElmer Spectrum RX l FT-IR Spectrometer Perkin Elmer System. The dried fragments were first ground with an agate mortar and sifted through a 75µm sieve to ensure uniformity in particle size. Then, the powders were mixed with potassium bromide (KBr) at a ratio of 1:100 by weight and ground gently by agate mortar to homogenize it before being poured in the sample holder as shown in **Fig.3. 10**. The agate mortar was washed after each sample with diluted hydrochloric (HCl) acid and then isopropanol **Fig.3. 11**. The samples were scanned in the range of 450cm^{-1}-4000cm^{-1} with a resolution of 4cm^{-1}, by taking 16 scans for each measurement.

(a)

(b)

Fig.3. 10. FTIR (a) machine and (b) sample holder.

Fig.3. 11. Agate mortar cleaning in the fume hood with diluted HCl acid and isopropanol.

3.5.7.3. Scanning Electron Microscopy

The microstructure of the samples at 28d and after 108 cycles was analyzed using a Zeiss Evo Ma15 Scanning Electron Microscope (SEM), **Fig.3. 12**(a), with a wide range of detectors. The tests were conducted at an accelerating voltage of 10kV and a low vacuum (EP mode) at around 30 Pa which allows analyzing nonconductive dry samples [43]. Nitrogen (N_2) was used to reduced charging of the samples. The dried fragments were placed directly on metal stubs without a sticky tape as shown in **Fig.3. 12**(b) and examined at different magnifications ranging from 500x to 5000x without any metal or carbon coating.

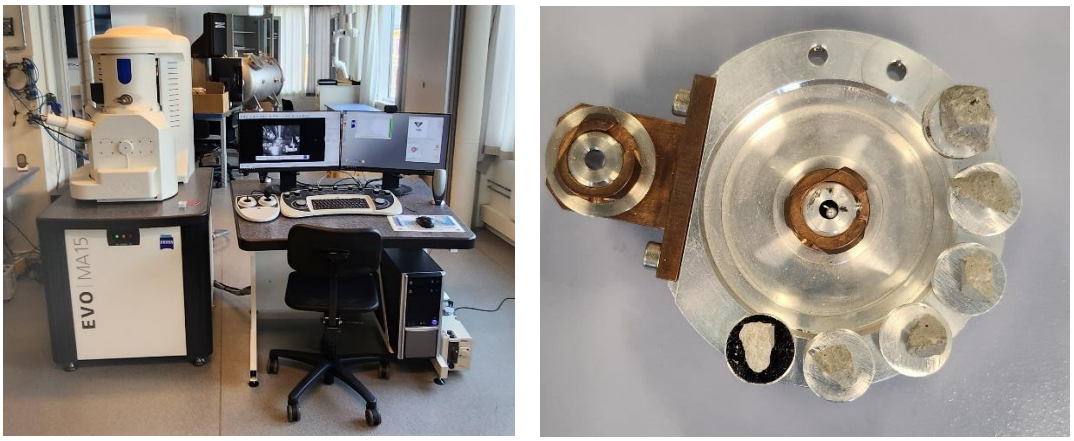

(a) (b)

Fig.3. 12. (a) SEM and (B) samples on the sample holder.

‘

Chapter 4: Results and discussion

4.1. Introduction.

This chapter presents the results of tests conducted on slump and spread, hardened properties, and microstructural analysis. The data was carefully analyzed, and a comprehensive comparison was performed. The objective of conducting these tests was to gain a deeper understanding of the subject matter compared to the existing researches conducted by other scholars.

4.2. Slump and spread.

Results of slump and spread are shown in **Fig.4. 1**. For slump test, samples with seawater exhibited higher value than samples with fresh water except for the sample PW_2 and SW_2. These two samples with (80% cement, 10% SF and 10% FA), showed opposite results compared to the rest of the samples. However, seawater is known to reduce the slump and flow value when it mixed with cement's paste in accordance with other literature such as in [7], [28]. This error can be due to the unappropriated mixer available at OsloMet's lab.

For spread test, samples mixed with freshwater exhibits higher value than samples mixed with freshwater except for PW_2 and SW_2. These two samples with (80% cement, 10% SF and 10% FA), showed opposite results compared to the rest of the samples. This adverse results for these two samples in both spread and slump test can be due to FA and SF.

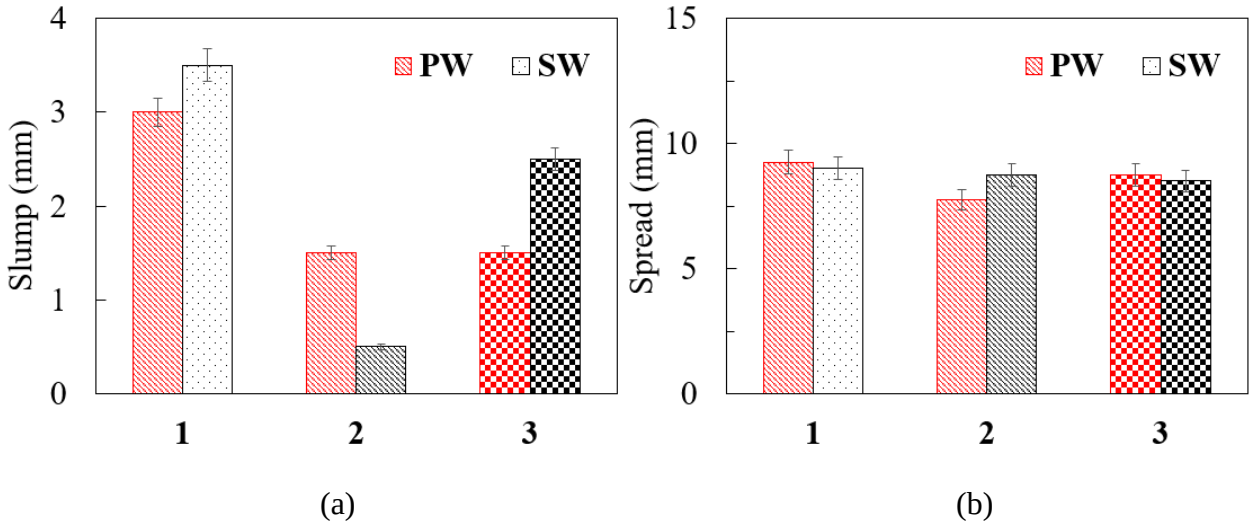

Fig.4. 1. (a) Slump test results. (b) Flow value results.

4.3. Hardened properties.

4.5. Compressive strength

4.5.1. Compressive strength of samples cured in water.

At **Fig.4. 2**, for the SW samples, the compressive strength ranged from 22.3 MPa to 56.1 MPa over the 56-day period. Initially, at 3 days, SW1 exhibited the highest strength of 46.5 MPa, which decreased slightly to 31.9 MPa at 56 days. SW2 showed a changing trend, starting at 38.5 MPa and reaching a minimum of 37.0 MPa at 56 days. On the other hand, SW3 displayed an increasing trend in compressive strength, starting at 22.3 MPa and reaching a peak of 56.1 MPa at 56 days.In the case of the PW samples, the compressive strength ranged from 25.9 MPa to 54.3 MPa over the 56-day period. PW1 exhibited a decreasing trend in strength, starting at 39.8 MPa and reaching a minimum of 33.2 MPa at 28 days, followed by a slight recovery to 37.3 MPa at 56 days. PW2 displayed an increasing trend, starting at 40.4 MPa and peaking at 54.3 MPa at 28 days, followed by a slight decline. PW3 showed relatively consistent strength throughout the period, starting at 25.9 MPa and ending at 33.1 MPa at 56 days. Comparing the SW and PW samples, it is evident that the PW samples generally exhibited higher compressive strength than the SW samples. However, the trend in compressive strength varied within each group of samples. Although at ages of 3 and 28d, SW1 samples exhibited higher strength compared to PW1 samples. This can be due to the effect of seawater on the hydration of specimens at the early ages.

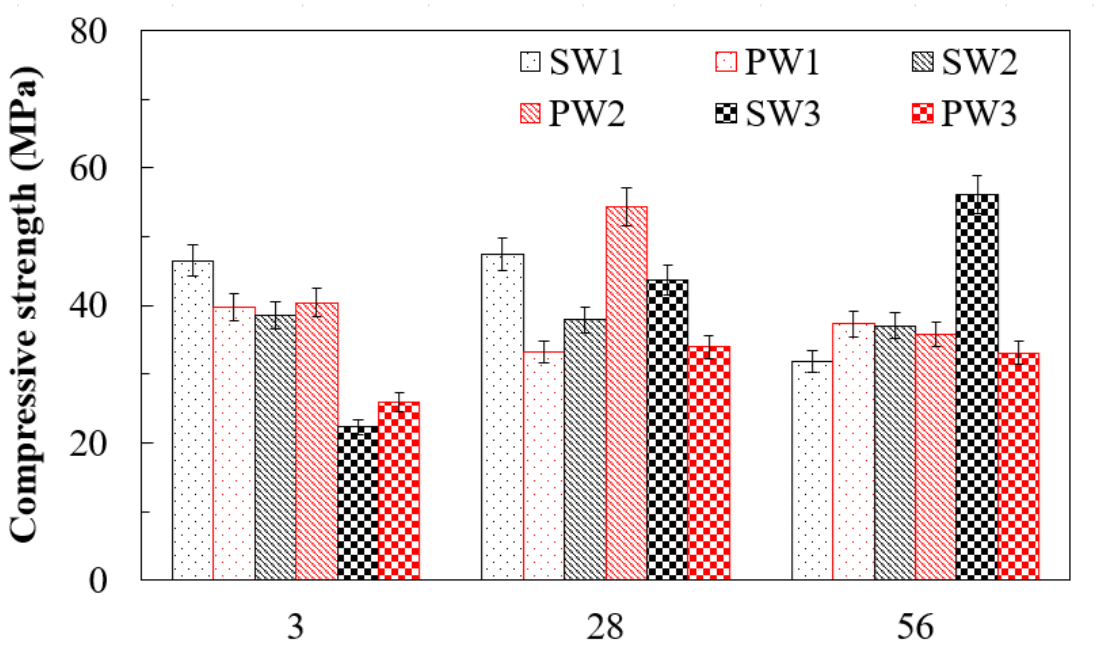

Fig.4. 2. Compressive strength of 3, 28 and 56d samples.

4.5.2. Compressive strength of samples with 36, 72 and 108 freeze-thaw cycles.

At **Fig.4. 3**. SW1's compressive strength rises from 37 MPa after 36 cycles to 63 MPa after 72 cycles, then falls slightly to 56 MPa after 108 cycles. This suggests an initial increase in strength, most likely owing to the continuous hydration process, but a subsequent fall caused by freez-thaw cycles. SW2 follows a similar pattern, with compressive strength increasing from 42 MPa after 36 cycles to 58 MPa after 72 cycles, then decreasing to 48 MPa after 108 cycles. This pattern is similar to SW1, but with a lower overall strength level. In terms of compressive strength, SW3 exhibits a declining tendency. After 36 cycles, the strength drops to 38 MPa, then 52 MPa after 72 cycles, and finally 39 MPa after 108 cycles. This indicates a greater susceptibility to freeze-thaw degradation, resulting in a considerable loss of strength over time.

PW1's compressive strength is 43 MPa after 36 cycles, then rising to 52 MPa after 72 cycles, and then decreasing to 39 MPa after 108 cycles. Throughout the testing time, the sample exhibits a changing strength performance. PW2's compressive strength decreases somewhat after 36 cycles, from 53 MPa to 45 MPa after 72 cycles, and then to 41 MPa after 108 cycles. Despite the decrease, the strength remains rather strong when compared to the other samples. PW3 has a changing pattern, with compressive strength decreasing from 40 MPa after 36 cycles to 45 MPa after 72 cycles, then increasing slightly to 44 MPa after 108 cycles. This suggests a mixed reaction to the freeze-thaw cycles.

The compressive strength of seawater samples (SW1, SW2, and SW3) after 36 cycles, exhibits a higher strength compared to freshwater samples (PW1, PW2, and PW3). This shows that under freeze-thaw circumstances, seawater may have a positive impact on the compressive strength of the samples.

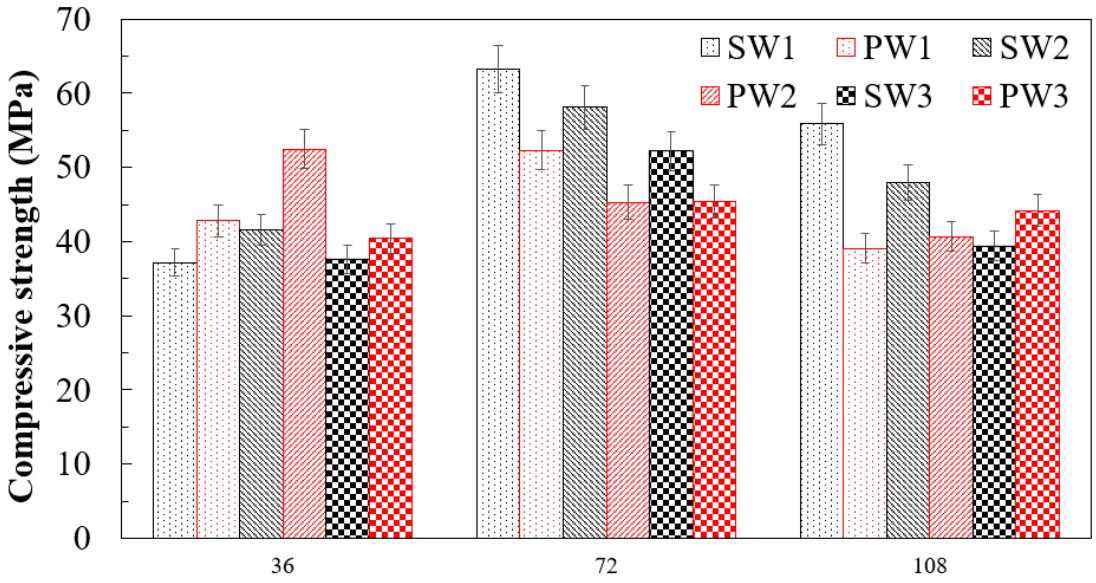

Fig.4. 3. Compressive strength after 36, 72 and 108 freeze-thaw cycle.

4.3.1. Water absorption and void space ratio result for samples cured in water at 3 days.

At **Fig.4. 4** (a). SW1 exhibits an absorption value of 22.395% after immersion, which corresponds to a volume of permeable pore space of 36.131%. This suggests that SW1 has relatively higher capacity to absorb a significant amount of water, resulting in a relatively high volume of permeable pore space. SW2 exhibits a lower absorption value of 15.873%, resulting in a 27.115% volume of permeable pore space. This shows that the sample has a lower water absorption capacity and a smaller amount of permeable pore space than SW1. This can be due to the reaction of SF and FA in the sample. SW3 has a similar pattern to SW2, with an absorption value of 16.494% and a permeable pore space volume of 27.760%. This implies that SW3 has a comparable water absorption capacity and amount of permeable pore space to SW2.

PW1 exhibits an absorption value of 21.861%, corresponding to a volume of permeable pore space of 36.305%. This indicates a high-water absorption capacity and a relatively high volume of permeable pore space within the sample, similar to SW1 with only small lesser absorption capacity compared to SW1. PW2 exhibits a lower absorption value of 16.140%, resulting in a volume of permeable pore space of 27.545%. This suggests a lower water absorption capacity and a reduced volume of permeable pore space within the sample compared to PW1. With an absorption value of 15.750% and a volume of permeable pore space of 26.337%, PW3 follows a similar pattern to PW2. This suggests that PW2 has a similar water absorption capacity and volume of permeable pore space.

Moreover, seawater (SW) samples compared to freshwater (PW) samples, seawater samples exhibit somewhat higher absorption values and volume of permeable pore space. This might be due to the presence of salts or minerals in saltwater, which could alter water absorption and the formation of porous pore spaces in concrete.

At **Fig**.4. 4.(a) Absorption **vs volume. (b) compressive strength** vs volume.(b). SW1 has the maximum compressive strength of 46.5 MPa and the highest volume of permeable pore space of 36.131%. This indicates that, despite the existence of void spaces, the sample has a reasonably high compressive strength. SW2 has a slightly lower compressive strength of 38.5 MPa and a permeable pore space volume of 27.1%. This indicates a lower compressive strength than SW1, it is probably due to the greater amount of void in the sample. SW3 has the lowest compressive strength of any seawater sample, at 22.3 MPa. The permeable pore space volume is 27.7 %. PW1 has a compressive strength of 39.8 MPa, and a volume of permeable pore space of 36.3%. PW2 has a compressive strength of 40.4 MPa, which is comparable to PW1, but has a little smaller volume of permeable pore space of 27.5%. This suggests that the amount of voids has a minimal influence on compressive strength in freshwater samples, as it does in seawater samples. PW3 has a compressive strength of 25.9 MPa, and a volume of permeable pore space of 26.337%.

When seawater (SW) samples are compared to freshwater (PW) samples, the compressive strength values differ. The existence of voids has a greater influence on compressive strength in seawater samples mixed with SF and FA than in freshwater samples.

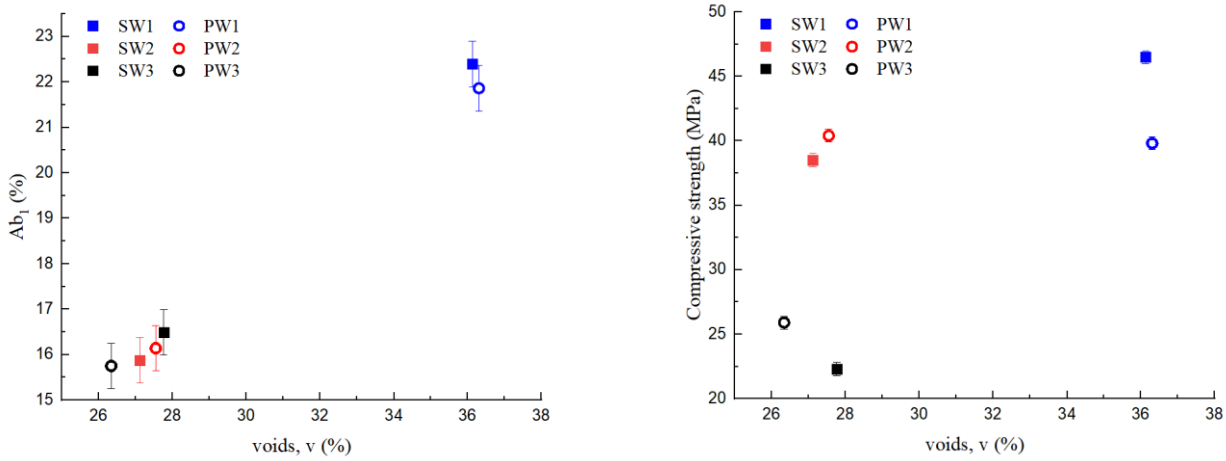

a b

Fig.4. 4.(a) Absorption vs volume. (b) compressive strength vs volume.

At **Fig.4. 5**. Among the freshwater (PW) samples, PW1 exhibits the highest apparent density value of 2.56 Mg/m^{3}This indicates a higher packing density compared to the seawater samples SW1 and SW2 with a density 2.50 Mg/m^{3}and 2.25 Mg/m^{3,} respectively. PW2 exhibits a slightly lower apparent density value of 2.27 Mg/m^3, suggesting a relatively lower packing density compared to PW1. PW3 exhibits the lowest apparent density among the freshwater samples, measuring 2.19 Mg/m^3. This indicates that the particles within PW3 are less densely packed compared to both PW1 and PW2 and also SW3 with a measured density of 2.22 Mg/m^3.

SW1 and PW1 have the highest apparent densities in these results, indicating denser particle packing and perhaps higher mechanical qualities. SW3 and PW3 have the lowest apparent densities, indicating a looser packing and perhaps lower strength.

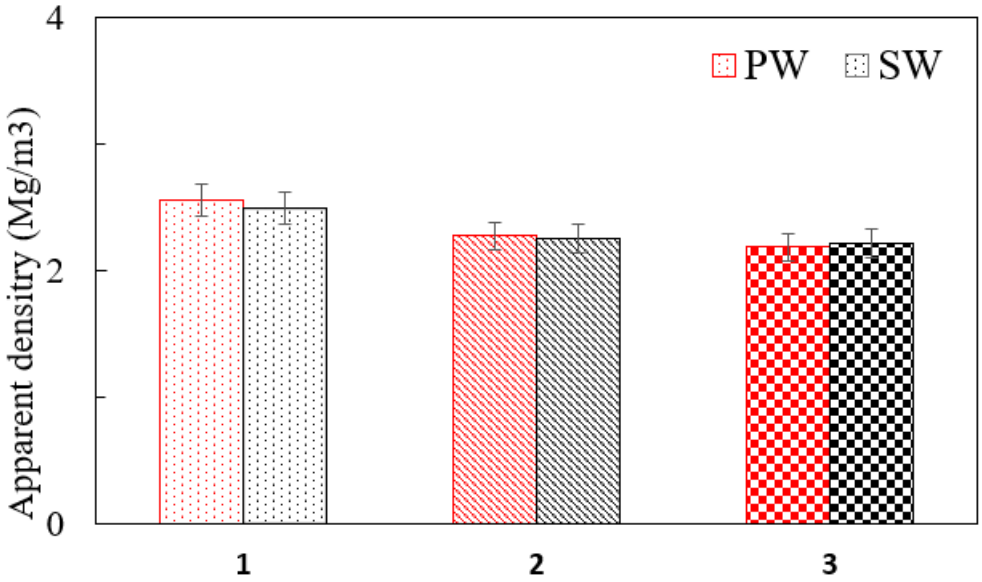

Fig.4. 5. Apparent density.

4.3.2. Water absorption and void space ration for samples cured in water at 28 days.

At **Fig.4. 6**.(a). SW1 had the greatest absorption following immersion of any of the seawater (SW) samples, at 22.5%, which is mirrored in its somewhat bigger amount of permeable pore space, at 28.2%. SW1 appears to have more porosity and permeability, allowing more water to infiltrate the sample. SW2 and SW3 have somewhat lower absorption percentages than SW1, indicating a reduced water intake. This corresponds to their volume of

permeable pore space values of 23.7% and 22.5%, respectively. These findings indicate that SW2 and SW3 have somewhat lower porosity and permeability than SW1.

PW1 had the largest absorption after immersion (21.8%) of the freshwater (PW) samples, which corresponds to its bigger amount of permeable pore space (26.0%). This suggests that PW1 has more porosity and permeability. PW2 and PW3 had lower absorption percentages than PW1, suggesting poorer water absorption and, as a result, lesser amounts of permeable pore space at 23.2% and 21.2%, respectively. These findings indicate that PW2 and PW3 have reduced porosity and permeability.

At **Fig.4. 6** SW1 has the maximum compressive strength at 47.5 MPa, demonstrating that it has strong overall strength. It also has a greater amount of permeable pore space (28.1%), indicating moderate porosity and permeability. SW2 has a slightly lower compressive strength of 37.9 MPa than SW1, suggesting that it is weaker. However, it has a lesser volume of permeable pore space at 23.6%, indicating a lower porosity and permeability. SW3 has a compressive strength of 43.7 MPa, which is between SW1 and SW2. It has a 22.5% volume of permeable pore space, showing a somewhat lower porosity and permeability than SW2.

PW1 has a compressive strength of 33.2 MPa, which is lower than the compressive strength of other seawater samples. It has a considerably greater amount of permeable pore space (26.0%) than seawater samples, indicating higher porosity and permeability.PW2 has the maximum compressive strength of any sample, measuring 54.3 MPa, showing outstanding strength. It also has a lesser volume of permeable pore space (23.2%), implying poorer porosity and permeability. PW3 has a compressive strength of 33.9 MPa. It has the smallest amount of permeable pore space (21.1%), implying the lowest porosity and permeability of all of the samples.

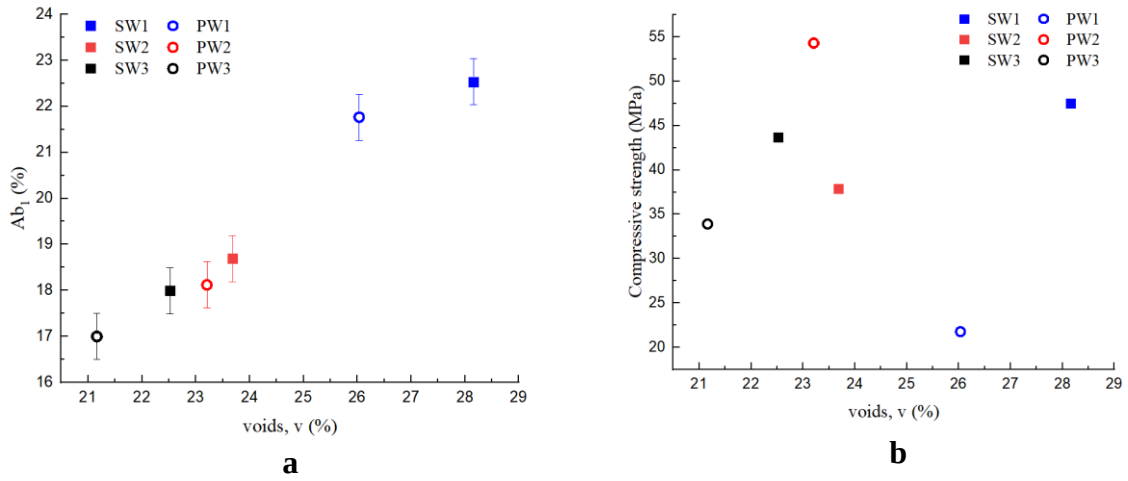

Fig.4. 6. (a) Absorption vs volume. (b) compressive strength vs volume.

At **Fig**.4. 7. Apparent density. SW1 exhibits an apparent density of 1.68 Mg/m^3, SW2 has a density of 1.58 Mg/m^3, and SW3 has a density of 1.53 Mg/m^3. PW1 has an apparent density of 1.58 Mg/m^3, PW2 has a density of 1.60 Mg/m^3, and PW3 has a density of 1.48 Mg/m^3.

In general, seawater samples have greater apparent density values than freshwater ones. SW1 had the highest apparent density of any of the samples, measuring 1.68 Mg/m^3, indicating a denser and more compact concrete. PW3 had the lowest apparent density of all the samples, at 1.48 Mg/m^3, indicating a less dense and more porous concrete. The apparent density values of the other Seawater(SW2, SW3) and freshwater (PW1, PW2) samples are quite close.

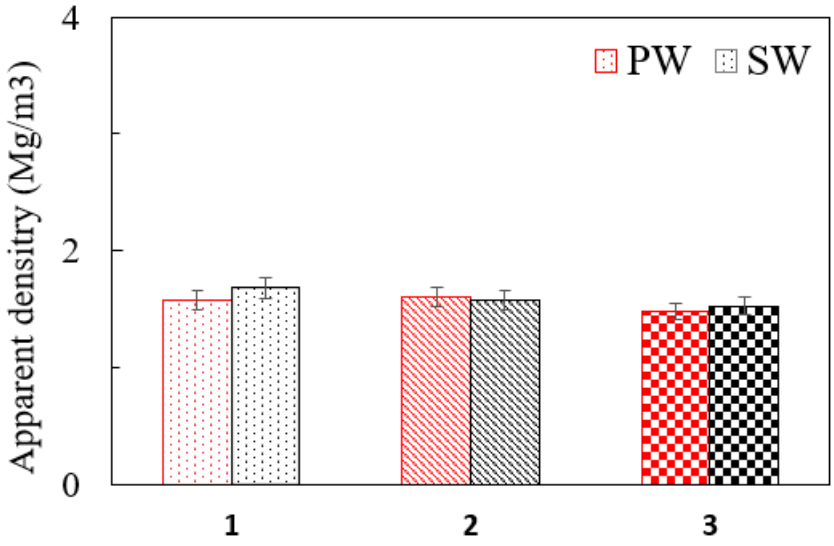

Fig.4. 7. Apparent density.

4.3.3. Water absorption and void space ration for samples after 72 freeze-thaw cycles.

At **Fig**.4. 8 .Absorption vs **volume.**. SW1 has a 21.6% absorption after immersion and a 23.3% amount of permeable pore space. This suggests that the porosity and permeability are modest. SW2 absorbs 16.5% and has a volume of permeable pore space of 21.3%. It implies that it has lower porosity and permeability than SW1. SW3 has a similar porosity and permeability to SW2 with an absorption of 17.1% and a volume of permeable pore space of 21.5%

PW1 had the largest absorption after immersion (22.4%) and the biggest amount of permeable pore space (27.2%). When compared to seawater samples, this indicates a higher amount of porosity and permeability. PW2 absorbs 16.5% and has a permeable pore space volume of 21.0%. It has the same porosity and permeability properties as SW2 and SW3. PW3 absorbs 17.3% and has a volume of permeable pore space of 21.7%, which is comparable to seawater samples. It implies a similar amount of porosity and permeability.

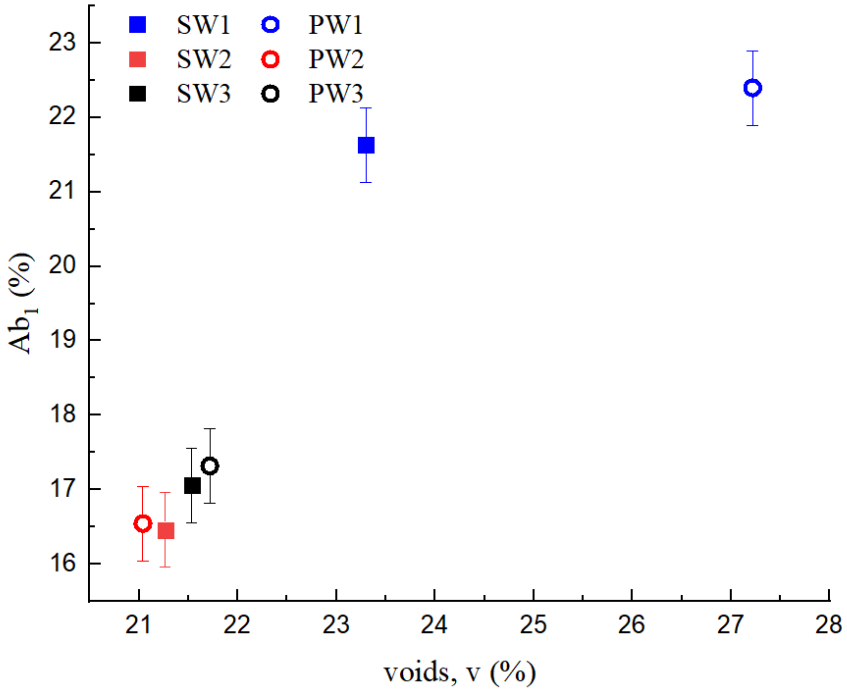

Fig.4. 8 .Absorption vs volume.

At **Fig.4. 9**. SW1 has an apparent density of 1.37 Mg/m^3, SW2 has 1.52 Mg/m^3, and SW3 has 1.51 Mg/m^3.PW1 has an apparent density of 1.64 Mg/m^3, PW2 has 1.51 Mg/m^3, and PW3 has 1.51 Mg/m^3.

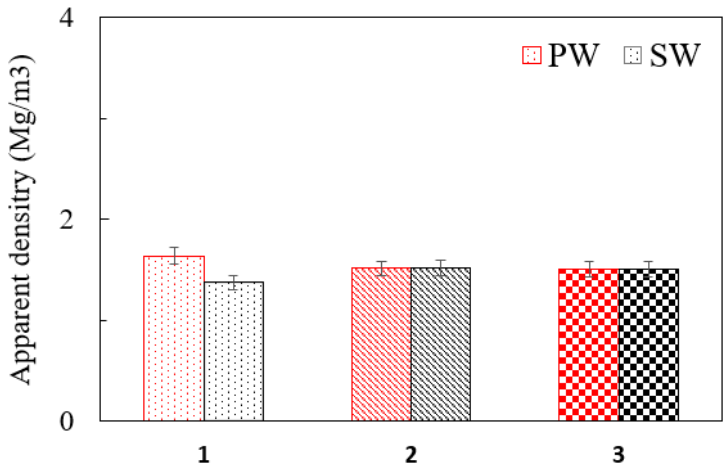

Fig.4. 9. Apparent density.

4.4. Freeze thaw test.

At **Fig.4. 10**, SW1 exhibits a weight loss of 60.00% after 36 cycles, which decreases to 30.00% after 72 cycles, and then slightly increases to 40.00% after 108 cycles. This indicates a fluctuating weight loss pattern but with an overall decreasing trend over time. SW2 exhibited consistent weight loss percentages of 60.00% after 36 cycles, 50.00% after 72 cycles, and 40.00% after 108 cycles. The sample maintains a relatively stable weight loss pattern. SW3 shows an increasing trend in weight loss. It starts at 70.00% after 36 cycles, increases to 60.00% after 72 cycles, and reaches 100.00% after 108 cycles. This suggests a higher vulnerability of the sample to freeze-thaw damage.

PW1 exhibits a weight loss of 40.00% after 36 cycles, which increases to 70.00% after 72 cycles, and then slightly decreases to 50.00% after 108 cycles. The sample demonstrates an increasing trend followed by a slight decrease in weight loss. PW2 exhibits consistent weight loss percentages of 50.00% after 36 cycles, 60.00% after 72 cycles, and 60.00% after 108 cycles. The sample maintains a relatively stable weight loss pattern. PW3 displays a fluctuating weight loss pattern. It starts at 30.00% after 36 cycles, increases to 80.00% after 72 cycles, and then decreases to 60.00% after 108 cycles.

In general, seawater samples had larger weight loss percentages than freshwater samples, indicating a possibly higher sensitivity to freeze-thaw damage. This is due to the presence of salts or minerals in seawater, which can lead to cement degradation.

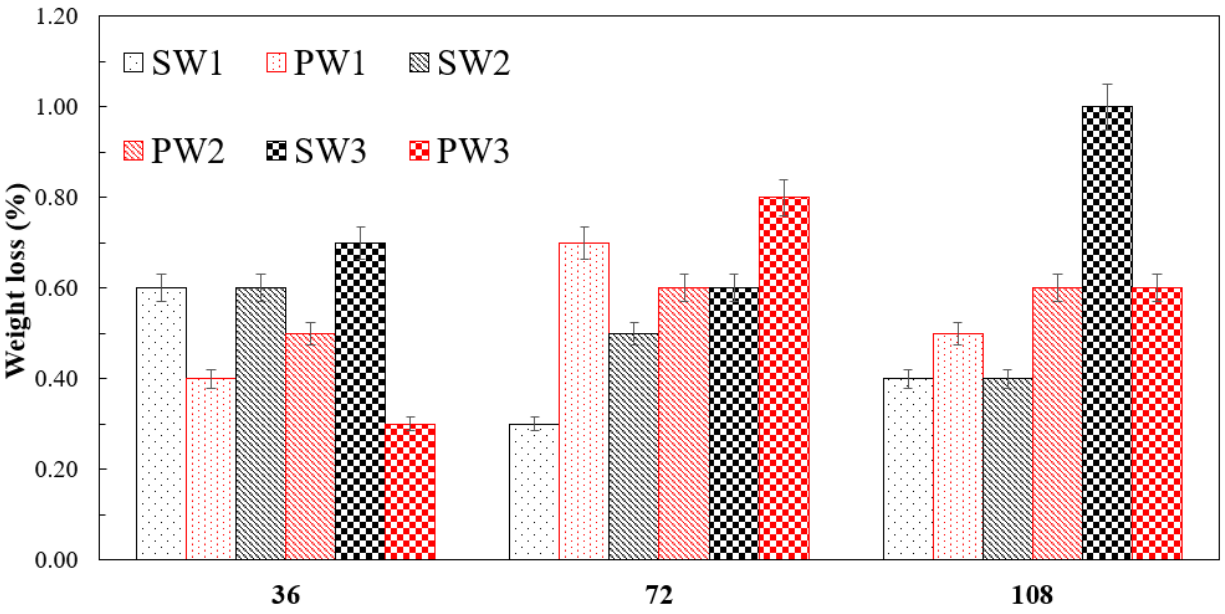

Fig.4. 10. Weight loss results for samples after 36,72 and 108 cycles.

4.6. Microstructural.

4.6.1. FTIR

Fig.4. 11 is the main contributor for analyzing the result's spectra. At **Fig.4. 12**, the symmetric and asymmetric stretching of the O-H vibrator of the water molecules causes the broad band visible in the range 3100 to 3550 cm^{-1}. The peak at 3644 cm^{-1} is one of the characteristics of portlandite. The band at 1074 cm^{-1} indicates present SO^{2-}_4 ions, this is one of the characteristics of ettringite reactions. This may be an indication for the higher compressive strength for SW1 at 28d compared to sample at 3d. However, this range for the samples mixed with binders such as FA and SF, indicates the presence of polymerized silica. Furthermore studies indicates that intensity for this band for cement-based materials without additives will decrease with hydration time increasing [44]. However, peaks for the both samples are almost identical.

Wave number [cm^{-1}]	Possible assignment	Reference
656–658	υ_4 of SiO_4	[21,40]
714	υ_4 of CO_3	[22,32,35,37]
847–848	Al–O, Al–OH	[21,35]
877–878	υ_2 of CO_3	[21,22,35,37]
1011–1080	Polymerized silica	[19]
~1100–1200	υ_3 of SO_4	[19,22,31,32]
1200–1202	Syngenite, thenardite	[32–34]
1400–1500	CO_3	[19,21,22,35,37]
1620–1624	υ_2 of water in sulphates	[22,31,33]
1640–1650	υ_2 H_2O	[21,35,36]
1682–1684	υ_2 of water in sulphates	[22,31,33]
1795–1796	$CaCO_3$	Own measurement, [22]
2513–2514	$CaCO_3$	Own measurement, [22]
2875–2879	$CaCO_3$	Own measurement, [22]
2983–2984	$CaCO_3$	Own measurement, [22]
3319–3327	Syngenite, thenardite	[32–34]
3398–3408	υ_3 of H_2O, capillary water	[36]
3457	$\upsilon_1 + \upsilon_3$ of H_2O	[21,36]
3554	υ_3 of H_2O in gypsum	[22,31]
3611	Bassanite	[22]
3641–3644	$Ca(OH)_2$	Own measurement, [20,23

a

Peaks used for the fitting of C_3S hydration difference spectra.

Spectral position	Component	Notes or reference
807 cm^{-1}	C-S-H Q^1-species	[16,17]
828 cm^{-1}	C_3S	Synthesized monoclinic C
878 cm^{-1}	C_3S	Synthesized monoclinic C
919 cm^{-1}	C_3S	Synthesized monoclinic C
944 cm^{-1}	C-S-H Q^2-species	970 cm^{-1} [16,17]
961 cm^{-1}	C_3S	Synthesized monoclinic C
976 cm^{-1}	Silanol groups	[19–21]
1007 cm^{-1}	C-S-H Q^1-species	This study
1059 cm^{-1}	C-S-H Q^2-species	[16,22]
1105 cm^{-1}	C-S-H Q^2-species	[16,22]

b

Wave number (cm^{-1})	Functional group
448–463	v_2 of SiO_4^{-2}
520–540	v_4 of SiO_4^{-2}
601	v_3 of SO_4^{-2}
664	$v_4$of SO_4^{-2}
1100–1200	v_4 of SO_4^{-2}
1400–1500	v_3 of CO_3^{-2}
1620–1624	V_2 of water in sulfate
1640–1650	V_2 of H_2O
1700–1800	$CaCO_3$
2875–2984	$CaCO_3$
3440–3450	$v_1 + v_3$ of H_2O

Fig.4. 11.(a) Possible assignment to some of the peaks [45], (b) infrared spectroscopy correlation table for C3S [46]. (c) wave number and functional group in FTIR spectra of cement [47].

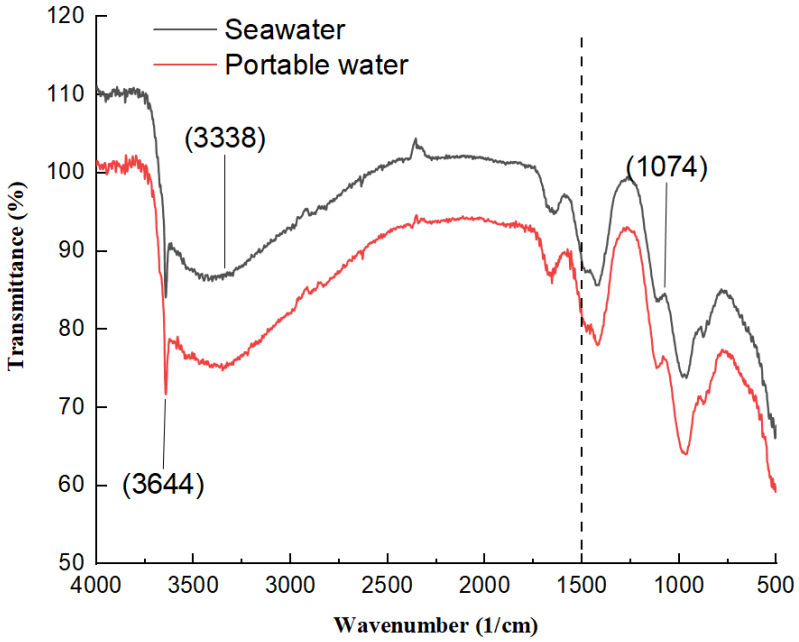

Fig.4. 12. FTIR For samples cured in water at 28d.

At **Fig.4. 13**, OH(CH) reaction observed for all of the samples in the range of 3500-3550 Cm^{-1} . The broader range for the OH(H_2O) have been also observed for all of the samples at the age of 28 days in the range of 3000 to 3500 Cm^{-1}.

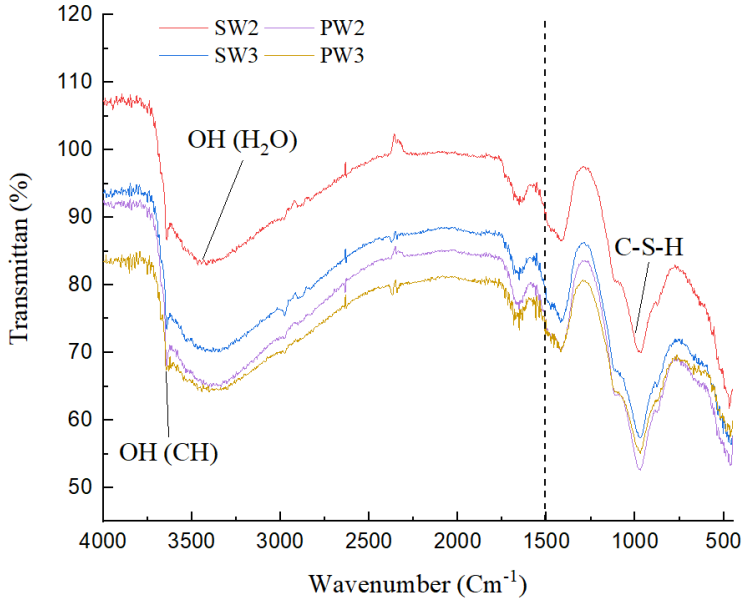

Fig.4. 13. FTIR For samples cured in water at 28d.

Fig.4. 14, shows the FTIR spectra of cement, FA and SF. Cement and fly ash exhibits similarity in the curve structure, however silica fume exhibiting more volatile peaks compared to others. This may be dude to error in the sample analysis.

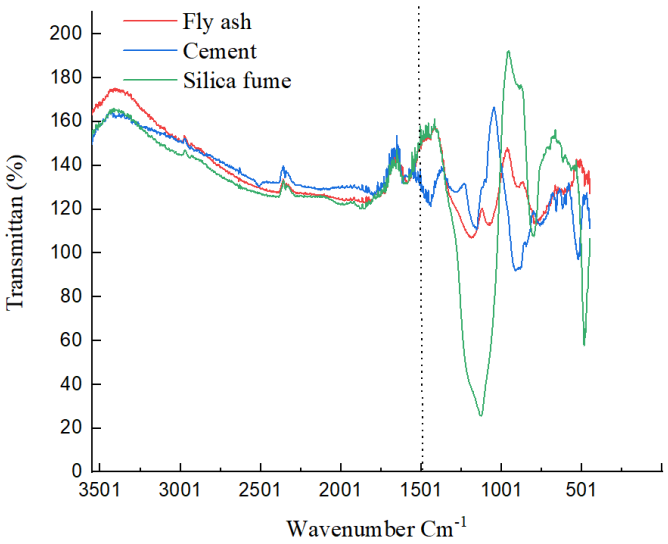

Fig.4. 14. FTIR of Cement, FA and SF.

4.6.2. SEM.

4.6.2.1. SEM analysis for samples at the age of 28.

At **Fig.4. 15**. SW1 Exhibits rougher surface compared to PW3 sample. The yellow cycle for SW1 sample may indicate the presence of Friedel's salt. Spherical shape figures in both PW2 and SW2 samples is an indication of FA presence.

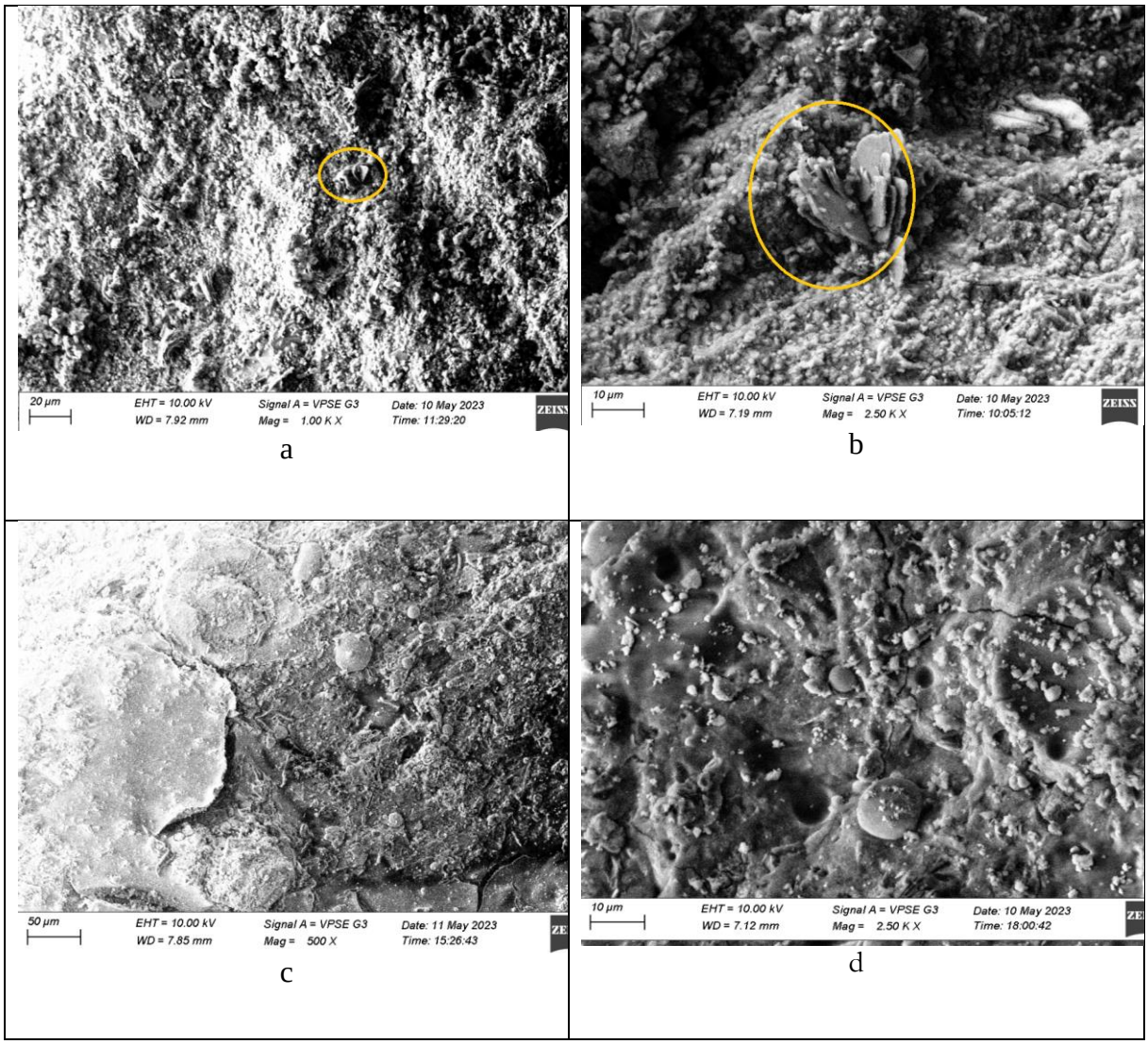

Fig.4. 15. (a) SW1 sample 1.00K.X, (b) SW1 samples 2.50 KX, (c) PW3 500X and (d) SW2 2.50KX.

4.6.2.2. SEM analysis for samples After 72 cycles.

Fig.4. 16, demonstrating SEM photos of camples after 72 freez-that cycles. The yellow circled on Fig 4 19 (a), may indicate the ettringite reaction in the sample [48]. Red highlighted cycles in the sample PW2, indicates the presence of FA, however as it shown in the picture. Smooth surface on the shape may indicates that FA didn't fully react after 72 cycles of freeze-thaw. The same observation is been made for SW3 samples.

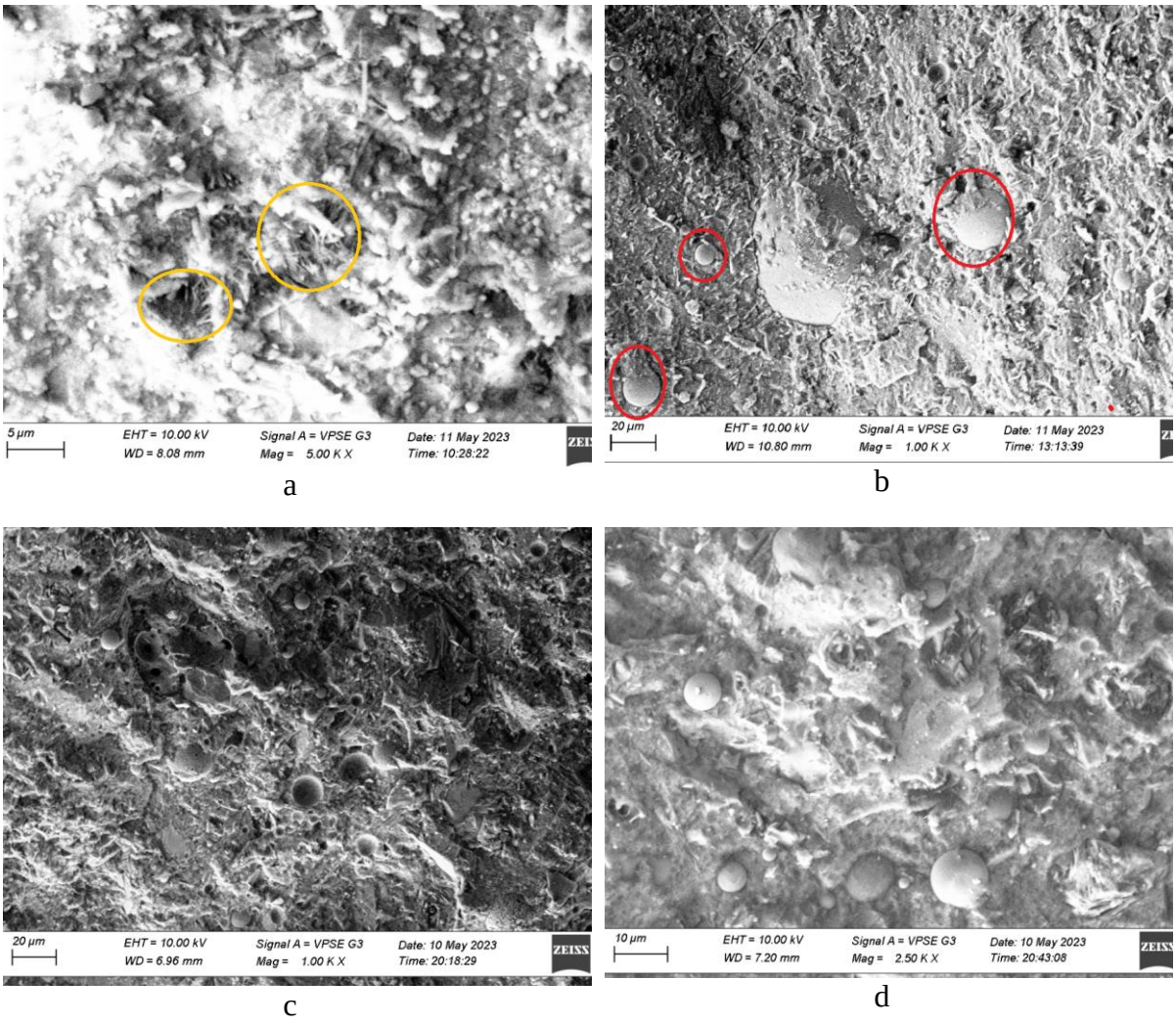

Fig.4. 16. (a) PW1 5.00 KX, (b) PW2 1.00KX,(c) SW3 1.00 KX and (d) SW3 2.50 KX.

4.6.2.3. SEM analysis for samples After 108 cycles.

Fig.4. 17, demonstrating SEM photos of PW1 sample after 108 cycles of freeze-thaw. The yellow highlighted area in picture may indicate ettringite reaction. Somehow there is uncertainty due to the bad quality of picture. Red highlighted cycles in the second picture may indicate the presence of portlandite salt in the sample.

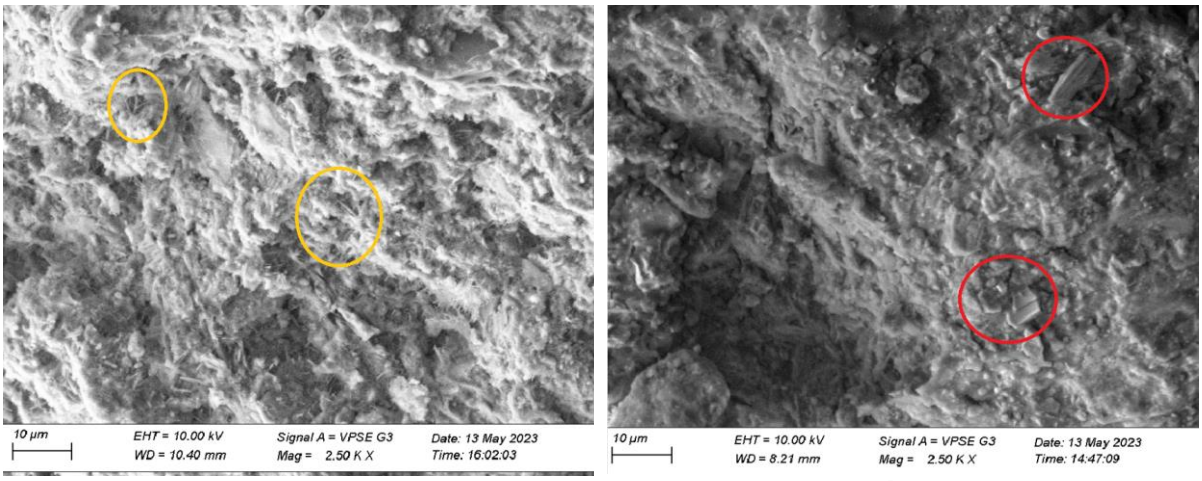

a b

Fig.4. 17. PW1 2.50KX.

Chapter 5: Conclusion and future work:

Following research questions have been answered in this thesis.

(1) What is already known about the individual and combined effect of SW, SF and FA on the properties of cement-paste?, by reviewing literature reviews, we found that FA and and Silica fume have detrimental effects on the hydration and the early age strength development on concrete. However, by conducting this test, SW3 mixed with FA and SF, showed promising results after 56 days. SW3 exhibited a higher strength compared to all other samples.

(2) (2) Can SCMs be beneficial for the compressive strength of a paste made with SW or will they introduce a more complex effect? The results of the compressive strength indicated that sample SW3 with (70% cement, 10% SF and 20% SF), exhibited the highest strength compared to other samples after 56 days. This may be a good indication of the positive combined effect of Seawater and SCMs on the compressive strength. However, the results of weight loss after 108 freeze-thaw cycles. Indicated a highest weight for SW3 compared to other samples. This may be due to mineral and salt content in seawater which led to cement degradation.

(3) Which of the SF or SW exerts a dominant influence on the strength variation of the paste at an early age? At early ages, samples with freshwater mixed with binder exhibited a higher strength then as samples mixed with seawater and SCMs. This clearly indicates the dominant effect of SF at the early ages.

Following questions haven't been answered in this thesis:

1. Will the studied binder maintain its strength after undergoing multiple thermal cycling?
2. Is the microstructure sufficient to explain the strength variation of a paste containing both SCMs and SW?

By conducting these tests, conclusion is as follow**:**

1. In conclusion, the results of the slump and spread tests showed that, in general, samples mixed with seawater exhibited higher values compared to those mixed with freshwater, except for the PW2 and SW2 samples. However, this contradicts the common understanding that seawater reduces slump and flow values when mixed with cement paste. The discrepancy may be attributed to the limitations of the available mixer in the laboratory. Additionally, the inclusion of fly ash (FA) and silica fume (SF) in the PW2 and SW2 samples may have influenced the adverse results in both the spread and slump tests.
2. The absorption and permeable pore space results indicate that the seawater (SW) samples, particularly SW1, have a higher water absorption capacity and a larger volume of permeable pore space compared to the freshwater (PW) samples. This difference may be attributed to the presence of salts or minerals in seawater. In terms of compressive strength, SW1 exhibits the highest strength despite the presence of void spaces, while SW2 and SW3 show slightly lower compressive strength values. In contrast, the compressive strength of PW samples is less affected by the presence of voids. Overall, the influence of voids on compressive strength is more pronounced in seawater samples mixed with supplementary cementitious materials (SF and FA) than in freshwater samples.
3. The seawater (SW) samples exhibited varying weight loss percentages over the freeze-thaw cycles, with SW1 and SW3 showing fluctuating patterns and SW2 demonstrating consistent weight loss. On the other hand, the freshwater (PW) samples displayed increasing, stable, and fluctuating weight loss patterns for PW1, PW2, and PW3, respectively. Overall, the seawater samples exhibited higher weight loss percentages compared to the freshwater samples, indicating a potential higher vulnerability to freeze-thaw damage. This can be attributed to the presence of salts or minerals in seawater, which contribute to cement degradation.
4. The compressive strength of the seawater (SW) samples ranged from 22.3 MPa to 56.1 MPa over the 56-day period. SW1 initially had the highest strength but decreased slightly over time, while SW2 showed a changing trend and SW3 exhibited an increasing trend in compressive strength. For the freshwater (PW) samples, the compressive strength ranged from 25.9 MPa to 54.3 MPa. PW1 exhibited a decreasing trend, PW2 showed an increasing trend followed by a slight decline, and PW3 maintained relatively consistent strength. Overall, the PW samples generally displayed

higher compressive strength than the SW samples, although SW1 showed higher strength at early ages, possibly due to the effect of seawater on early hydration.

5. Results suggest that seawater may have a beneficial effect on the compressive strength of samples subjected to freeze-thaw cycles, as evidenced by the higher initial strength observed in the seawater samples compared to freshwater samples. However, the subsequent decrease in strength in the seawater samples indicates the potential degradation effects of freeze-thaw cycles. Further research and analysis are needed to understand the underlying mechanisms and optimize the use of seawater in enhancing the durability of concrete under freeze-thaw conditions.

Suggestion for the future study is as follow:

1. More in depth examination of the difference between slump and spread test results between seawater and freshwater specimens.
2. More in-depth examination of the effect of seawater in water absorption and permeable pore space.
3. More in-depth examination of freeze-thaw test with different SCM.
4. 4.more in depth examination of compressive strength and comparison between freshwater sample and seawater sample over longer extended periods of time.
5. more research on better understanding the of the underlying mechanisms and optimize the use of seawater in enhancing the durability of concrete.

Refences

[1] P. Li, W. Li, Z. Sun, L. Shen, and D. Sheng, "Development of sustainable concrete incorporating seawater: A critical review on cement hydration, microstructure and mechanical strength," *Cement and Concrete Composites*, vol. 121, p. 104100, 2021/08/01/ 2021, doi: https://doi.org/10.1016/j.cemconcomp.2021.104100.

[2] G. C. a. C. Association. "Cement and Concrete around the world " https://gccassociation.org/concretefuture/cement-concrete-around-the-world/ (accessed 23.5, 2023).

[3] U.N. "Access to freshwater " UN. https://www.un.org/sustainabledevelopment/water-and-sanitation/ (accessed 23/05, 2023).

[4] M. t. c. center, "Concrete Industry

Sustainability Performance

Report," 2020. [Online]. Available: https://www.sustainableconcrete.org.uk/MPA-ACP/media/SustainableCon-Media-Library/Pdfs%20-%20Performance%20reports/14th-146829-TCC-Performance-Report-A4-6pp-Prf6.pdf

[5] J. Xiao, C. Qiang, A. Nanni, and K. Zhang, "Use of sea-sand and seawater in concrete construction: Current status and future opportunities," *Construction and Building Materials*, vol. 155, pp. 1101-1111, 2017/11/30/ 2017, doi: https://doi.org/10.1016/j.conbuildmat.2017.08.130.

[6] R. G. Pillai, R. Gettu, and M. Santhanam, "Use of supplementary cementitious materials (SCMs) in reinforced concrete systems – Benefits and limitations," *Revista ALCONPAT*, vol. 10, no. 2, pp. 147-164, 2020, doi: 10.21041/ra.v10i2.477.

[7] L. G. Li, X. Q. Chen, S. H. Chu, Y. Ouyang, and A. K. H. Kwan, "Seawater cement paste: Effects of seawater and roles of water film thickness and superplasticizer dosage," *Construction and Building Materials*, vol. 229, p. 116862, 2019/12/30/ 2019, doi: https://doi.org/10.1016/j.conbuildmat.2019.116862.

[8] A. Witze, "Rare mineral is the key to long-lasting ancient concrete," *Nature*, 2017/07/03 2017, doi: 10.1038/nature.2017.22231.

[9] T. Dhondy, A. Remennikov, and M. N. Shiekh, "Benefits of using sea sand and seawater in concrete: a comprehensive review," *Australian Journal of Structural Engineering*, vol. 20, no. 4, pp. 280-289, 2019/10/02 2019, doi: 10.1080/13287982.2019.1659213.

[10] P. Sikora, K. Cendrowski, M. Abd Elrahman, S.-Y. Chung, E. Mijowska, and D. Stephan, "The effects of seawater on the hydration, microstructure and strength development of Portland cement pastes incorporating colloidal silica," *Applied Nanoscience*, vol. 10, no. 8, pp. 2627-2638, 2020/08/01 2020, doi: 10.1007/s13204-019-00993-8.

[11] A. Ghazal, M. El-Sheikh, and A. El-Rahim, "Effects of Seawater on Setting Time and Compressive Strength of Concretes with Different Richness," *Civil Engineering Journal*, vol. 7, pp. 857-865, 05/01 2021, doi: 10.28991/cej-2021-03091695.

[12] T. U. Mohammed, H. Hamada, and T. Yamaji, "Performance of seawater-mixed concrete in the tidal environment," *Cement and Concrete Research*, vol. 34, no. 4, pp. 593-601, 2004/04/01/ 2004, doi: https://doi.org/10.1016/j.cemconres.2003.09.020.

[13] A. Younis, U. Ebead, P. Suraneni, and A. Nanni, "Fresh and hardened properties of seawater-mixed concrete," *Construction and Building Materials*, vol. 190, pp. 276-286, 2018/11/30/ 2018, doi: https://doi.org/10.1016/j.conbuildmat.2018.09.126.

[14] K.-H. Yang, Y.-B. Jung, M.-S. Cho, and S.-H. Tae, "Effect of supplementary cementitious materials on reduction of CO2 emissions from concrete," *Journal of Cleaner Production*, vol. 103, pp. 774-783, 2015/09/15/ 2015, doi: https://doi.org/10.1016/j.jclepro.2014.03.018.
[15] K. De Weerdt and H. Justnes, "The effect of sea water on the phase assemblage of hydrated cement paste," *Cement and Concrete Composites*, vol. 55, pp. 215-222, 2015/01/01/ 2015, doi: https://doi.org/10.1016/j.cemconcomp.2014.09.006.
[16] K. De Weerdt, D. Orsáková, and M. R. Geiker, "The impact of sulphate and magnesium on chloride binding in Portland cement paste," *Cement and Concrete Research*, vol. 65, pp. 30-40, 2014/11/01/ 2014, doi: https://doi.org/10.1016/j.cemconres.2014.07.007.
[17] A. Benli, M. Karataş, and E. Gurses, "Effect of sea water and MgSO4 solution on the mechanical properties and durability of self-compacting mortars with fly ash/silica fume," (in English), *Construction and Building Materials*, Article vol. 146, pp. 464-474, 2017, doi: 10.1016/j.conbuildmat.2017.04.108.
[18] Y. Zhao, X. Hu, C. Shi, Q. Yuan, and D. Zhu, "Determination of free chloride in seawater cement paste with low water-binder ratio," *Cement and Concrete Composites*, vol. 124, p. 104217, 2021/11/01/ 2021, doi: https://doi.org/10.1016/j.cemconcomp.2021.104217.
[19] Y. Rhaouti, Y. Taha, and M. Benzaazoua, "Assessment of the Environmental Performance of Blended Cements from a Life Cycle Perspective: A Systematic Review," *Sustainable Production and Consumption*, vol. 36, pp. 32-48, 2023/03/01/ 2023, doi: https://doi.org/10.1016/j.spc.2022.12.010.
[20] P. Li *et al.*, "Hydration of Portland cement with seawater toward concrete sustainability: Phase evolution and thermodynamic modelling," (in English), *Cement and Concrete Composites*, Article vol. 138, 2023, Art no. 105007, doi: 10.1016/j.cemconcomp.2023.105007.
[21] K. Katano, N. Takeda, A. Shimmura, M. Hisada, and N. Otsuki, "Development and application of concrete using seawater and by-product aggregates," in *Sustainable Construction Materials and Technologies*, 2016, vol. 2016-August: International Committee of the SCMT conferences. [Online]. Available: https://www.scopus.com/inward/record.uri?eid=2-s2.0-85049785846&partnerID=40&md5=e842233345c1907bbf100321d7ae5b8c. [Online]. Available: https://www.scopus.com/inward/record.uri?eid=2-s2.0-85049785846&partnerID=40&md5=e842233345c1907bbf100321d7ae5b8c
[22] H. Li, N. Farzadnia, and C. Shi, "The role of seawater in interaction of slag and silica fume with cement in low water-to-binder ratio pastes at the early age of hydration," (in English), *Construction and Building Materials*, Article vol. 185, pp. 508-518, 2018, doi: 10.1016/j.conbuildmat.2018.07.091.
[23] O. Şimşek, H. Y. Aruntaş, İ. Demir, H. Yaprak, and S. Yazıcıoğlu, "Investigation of the Effect of Seawater and Sulfate on the Properties of Cementitious Composites Containing Silica Fume," *Silicon*, vol. 14, no. 2, pp. 663-675, 2022/01/01 2022, doi: 10.1007/s12633-021-01052-0.
[24] K. Khayat, M. Vachon, and M. C. Lanctôt, "Use of blended silica fume cement in commercial concrete mixtures," *ACI Materials Journal*, vol. 94, pp. 183-192, 05/01 1997.
[25] V. Yogendran, B. Langan, M. N. Haque, and M. A. Ward, "Silica Fume in High-Strength Concrete," *Materials*, vol. 84, pp. 124-129, 1987.
[26] V. Srivastava, A. Harison, P. Mehta, A. Pandey, and R. Kumar, "Effect of Silica Fume in Concrete," vol. 3297, pp. 15-16, 04/01 2007.

[27] Mansyur, A. A. Amiruddin, H. Parung, M. W. Tjaronge, and M. Tumpu, "Utilization of Sea Water to Production of Concrete in Terms of Mechanical Behavior," *IOP Conference Series: Earth and Environmental Science*, vol. 921, no. 1, p. 012068, 2021/11/01 2021, doi: 10.1088/1755-1315/921/1/012068.

[28] U. E. a. Adel Younis a, , Prannoy Suraneni b, Antonio Nanni, "Fresh and hardened properties of seawater-mixed concrete," (in English), *Science direct* p. 11, 2018, doi: https://doi.org/10.1016/j.conbuildmat.2018.09.126.

[29] N. Otsuki, T. Saito, and Y. Tadokoro, "Possibility of Sea Water as Mixing Water in Concrete," *Journal of Civil Engineering and Architecture*, vol. 6, pp. 1273-1279, 12/28 2012, doi: 10.17265/1934-7359/2012.10.002.

[30] R. Yu, Z. Wang, M. Sun, Z. Yu, E. Dong, and D. Fan, "Effect of natural zeolite on water distribution and migration in low water/binder cement-based composites (LW/B-CC) mixed with seawater: An experimental and computational investigation," *Construction and Building Materials*, vol. 379, p. 131242, 2023/05/23/ 2023, doi: https://doi.org/10.1016/j.conbuildmat.2023.131242.

[31] Q. Li, H. Geng, Y. Huang, and Z. Shui, "Chloride resistance of concrete with metakaolin addition and seawater mixing: A comparative study," *Construction and Building Materials*, vol. 101, pp. 184-192, 2015, doi: 10.1016/j.conbuildmat.2015.10.076.

[32] S. I. Choi, J. K. Park, T. H. Han, J. Pae, J. Moon, and M. O. Kim, "Early-age mechanical properties and microstructures of Portland cement mortars containing different admixtures exposed to seawater," (in English), *Case Stud. Constr. Mater.*, Article vol. 16, 2022, Art no. e01041, doi: 10.1016/j.cscm.2022.e01041.

[33] Z. Zhang, B. Zhang, and P. Yan, "Comparative study of effect of raw and densified silica fume in the paste, mortar and concrete," *Construction and Building Materials*, vol. 105, pp. 82-93, 2016/02/15/ 2016, doi: https://doi.org/10.1016/j.conbuildmat.2015.12.045.

[34] R. J. Davies-Colley, "Yellow substance in coastal and marine waters round the South Island, New Zealand," *New Zealand Journal of Marine and Freshwater Research*, vol. 26, no. 3-4, pp. 311-322, 1992/12/01 1992, doi: 10.1080/00288330.1992.9516526.

[35] "Physical Properties of Sea Water," (in English). [Online]. Available: https://publishing.cdlib.org/ucpressebooks/data/13030/6r/kt167nb66r/pdfs/kt167nb66r_ch03.pdf.

[36] E. A. Odd Henrik Sælen, "LECTURE NOTES

IN PHYSICAL OCEANOGRAPHY," (in English), p. 108, 1976. [Online]. Available: https://www.uio.no/studier/emner/matnat/geofag/nedlagte-emner/GEO1030/h17/undervisningsmateriale/oseanografi/kompendium-2016-1.pdf.

[37] *Standard Practice for High-Shear Mixing of Hydraulic Cement Pastes* ASTM-C1738/C1738M-19, A. S. f. T. a. Materials, 2019.

[38] K. Scrivener, R. Snellings, and B. Lothenbach, *A Practical Guide to Microstructural Analysis of Cementitious Materials*. 2015.

[39] *Standard Test Method for*

Resistance of Concrete to Rapid Freezing and Thawing 1, A. S. f. T. a. Materials, ASTM, 2008.

[40] Z. Tan, S. A. Bernal, and J. L. Provis, "Reproducible mini-slump test procedure for measuring the yield stress of cementitious pastes," *Materials and Structures*, vol. 50, no. 6, p. 235, 2017/10/19 2017, doi: 10.1617/s11527-017-1103-x.

[41] *Standard Test Method forDensity, Absorption, and Voids in Hardened Concrete*, A. S. f. T. a. Materials, ASTM, 2006.

[42] J. Zhang and G. W. Scherer, "Comparison of methods for arresting hydration of cement," *Cement and Concrete Research*, vol. 41, no. 10, pp. 1024-1036, 2011/10/01/ 2011, doi: https://doi.org/10.1016/j.cemconres.2011.06.003.
[43] P. Mestres, N. Pütz, S. Garcia Gómez de las Heras, E. G. Poblete, A. Morguet, and M. Laue, "The surface topography of the choroid plexus. Environmental, low and high vacuum scanning electron microscopy," *Annals of Anatomy - Anatomischer Anzeiger*, vol. 193, no. 3, pp. 197-204, 2011/05/01/ 2011, doi: https://doi.org/10.1016/j.aanat.2011.02.016.
[44] V. Sasnauskas, "Cement hydration with zeolite-based additive," *Chemija*, vol. 24, pp. 271-278, 01/01 2013.
[45] R. Ylmén, U. Jäglid, B.-M. Steenari, and I. Panas, "Early hydration and setting of Portland cement monitored by IR, SEM and Vicat techniques," *Cement and Concrete Research*, vol. 39, no. 5, pp. 433-439, 2009/05/01/ 2009, doi: https://doi.org/10.1016/j.cemconres.2009.01.017.
[46] J. Higl, D. Hinder, C. Rathgeber, B. Ramming, and M. Lindén, "Detailed in situ ATR-FTIR spectroscopy study of the early stages of C-S-H formation during hydration of monoclinic C3S," *Cement and Concrete Research*, vol. 142, p. 106367, 2021/04/01/ 2021, doi: https://doi.org/10.1016/j.cemconres.2021.106367.
[47] A. Bahari, A. Sadeghi-Nik, M. Roodbari, A. Sadeghi-Nik, and E. Mirshafiei, "Experimental and theoretical studies of ordinary Portland cement composites contains nano LSCO perovskite with Fokker-Planck and chemical reaction equations," *Construction and Building Materials*, vol. 163, pp. 247-255, 2018/02/28/ 2018, doi: https://doi.org/10.1016/j.conbuildmat.2017.12.073.
[48] J. Wang, J. Xie, Y. Wang, Y. Liu, and Y. Ding, "Rheological properties, compressive strength, hydration products and microstructure of seawater-mixed cement pastes," *Cement and Concrete Composites*, vol. 114, p. 103770, 2020/11/01/ 2020, doi: https://doi.org/10.1016/j.cemconcomp.2020.103770.